

STOCHASTIC RESPONSE OF TORSIONALLY COUPLED MULTISTOREYED BUILDINGS

A Thesis Submitted
in Partial Fulfilment of the Requirements
for the Degree of
MASTER OF TECHNOLOGY

by

Pavan Agarwal

to the

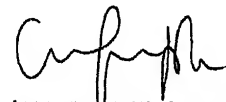
**DEPARTMENT OF CIVIL ENGINEERING
INDIAN INSTITUTE OF TECHNOLOGY KANPUR**

April 1993

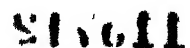
CERTIFICATE

IS. 4.93
(B)

It is certified that the work contained in the thesis entitled "Stochastic Response of Torsionally Coupled Multistoreyed Buildings" by "Pavan Agarwal" has been carried out under my supervision and that this work has not been submitted elsewhere for a degree.

 IS. 4.93

(VINAY KUMAR GUPTA)
Assistant Professor
Dept. of Civil Engineering
Indian Institute of Technology
Kanpur



CE 1893

TH
693.852
Ag 158

LIBRARY

Loc. No. A.115712

CE-1893-M-AGO-STO

*dedicated
to
my loving
parents and sisters*

ACKNOWLEDGEMENTS

First and foremost, I would like to express my deepest sense of gratitude to my teacher and advisor, Dr. V.K. Gupta for his constant help and encouragement, assiduous guidance and erudite suggestions throughout this endeavour. It was indeed a great pleasure and privilege for me to have been associated with him.

I am also indebted to all the faculty members of Civil Engineering Department, particularly to Dr. S.K. Jain, for their help and encouragement.

I am grateful to all my friends and well-wishers who made my stay here a memorable and pleasant experience. In particular, my sincere thanks go to K.V.S. Chandrasekher for his unstinted cooperation and help.

Last but not the least, I am really indebted to my parents and sisters. Their constant encouragement provided me the impetus to work with extra vigour.

TABLE OF CONTENTS

LIST OF TABLES	vii
LIST OF FIGURES	viii
ABSTRACT	x
CHAPTER I: INTRODUCTION	
1.1 General Introduction	1
1.2 Organization	6
CHAPTER II: FORMULATION OF STOCHASTIC APPROACH FOR TORSIONALLY COUPLED BUILDINGS	
2.1 Brief Review	8
2.2 Equations of Motion.....	11
2.3 Energy Spectra for the System Response.....	17
2.4 Nonstationarity in System Response	21
2.5 Illustration of the Proposed Model	23
CHAPTER III: DYNAMIC AMPLIFICATION OF ECCENTRICITY USING STOCHASTIC APPROACH	
3.1 Background	44
3.2 Dynamic Amplification of Eccentricity	44
3.3 Example Analysis	46
3.4 Parametric Dependence of Amplification Factor	52

3.5 Comparison with Indian Standard Code Provisions	54
CHAPTER IV: CONCLUSIONS	58
REFERENCES	60

LIST OF TABLES

2.1 Properties of First Example Building.	24
2.2 Properties of Second Example Building.	25
2.3 Natural Frequencies of First Example Building.	27
2.4 Natural Frequencies of Second Example Building.	28
3.1 Natural Frequencies of Torsionally Uncoupled Building.	47

LIST OF FIGURES

2.1 Multi-Degree-of-Freedom System for Torsionally Coupled Buildings.	12
2.2 i^{th} Floor Level of the Building.	14
2.3 Recorded Accelerogram at El Centro Site for Imperial Valley Earthquake, 1940, S00E Component.	29
2.4 Synthetic Accelerogram for Mexico Earthquake, 1985 at Mexico City Site.	29
2.5 Normalized Fourier Spectrum for Imperial Valley Earthquake.	30
2.6 Normalized Fourier Spectrum for Mexico Earthquake.	30
2.7 Normalized Displacement Responses in First Example Building for Imperial Valley Earthquake.	32
2.8 Normalized Shear Responses in First Example Building for Imperial Valley Earthquake.	33
2.9 Normalized Moment Responses in First Example Building for Imperial Valley Earthquake.	34
2.10 Normalized Displacement Responses in First Example Building for Mexico Earthquake.	35
2.11 Normalized Shear Responses in First Example Building for Mexico Earthquake.	36
2.12 Normalized Moment Responses in First Example Building for Mexico Earthquake.	37
2.13 Normalized Displacement Responses in Second Example Building for Imperial Valley Earthquake.	38
2.14 Normalized Shear Responses in Second Example Building for Imperial Valley Earthquake.	39
2.15 Normalized Moment Responses in Second Example Building for Imperial Valley Earthquake.	40
2.16 Normalized Displacement Responses in Second Example Building for Mexico Earthquake.	41

2.17 Normalized Shear Responses in Second Example Building for Mexico Earthquake.	42
2.18 Normalized Moment Responses in Second Example Building for Mexico Earthquake.	43
3.1 Effect of Floor to Floor Variation of Eccentricity on Amplification Factor.	49
3.2 Comparison of Amplification Factor in 1 and 8-Storey Building.	51
3.3 Comparison of Amplification Factor in 1 and 13-Storey Building.	51
3.4 Effect of Different Earthquake Excitations on Amplification Factor.	53
3.5 Variation of Amplification Factor with e_{yr} for Different ω_θ/ω_x values.	53
3.6 Variation of Amplification Factor with ω_θ/ω_x for Different e_y/r values.	55
3.7 Effect of e_{xr} on Amplification Factor for Different e_{yr} values.	55
3.8 Comparison of Amplification Factor with the Code Values.	57
3.9 Comparison of Amplification Factor for Higher Orders of Peak with the Code Values.	57

ABSTRACT

A stochastic approach based on response spectrum superposition technique has been formulated to determine the lateral-torsional response of torsionally coupled multistoreyed buildings subjected to the earthquake excitations. The eccentricity between the centre of mass and centre of resistance has been assumed to be the main cause of the lateral and torsional response of the building. This approach is quite general as it can estimate the response peaks for all orders with the given level of confidence while accounting for the cross-correlation between various modes of vibration.

By using the above approach, single storey models have been investigated for estimating the dynamic eccentricity values at different floor levels of a multistoreyed building. From these, parametric dependence of the dynamic eccentricity versus static eccentricity relationship has been shown more clearly, and it has been found that the codal provisions for torsional moments need to be thoroughly revised for more conservatism and rationality.

CHAPTER I

INTRODUCTION

1.1 General Introduction

Buildings are seldom, if ever totally symmetric. This asymmetry may occur due to the unsymmetrical distribution of mass and/or stiffness in the plan. Even in a structure whose geometry is symmetric, asymmetry is introduced by the variation in quality or method of construction, or by uncertainties in the live and dead load distribution. The buildings, which are asymmetric in plan or elevation due to their geometry or by the variation in mass and stiffness properties are called asymmetric buildings. This asymmetry in the buildings causes the positions of centre of mass and centre of resistance (also called as centre of stiffness or centre of rigidity) to be different. Quantitatively, this noncoincidence is expressed in terms of static eccentricity, i.e. the distance between the centre of mass and centre of resistance.

Based on the concept of static eccentricity, a torsionally-coupled building is defined as one in which the centre of mass and resistance in at least one storey are not coincident. So the inertial forces acting at the centre of mass and the elastic forces acting at the centre of resistance form a dynamic couple, which causes interdependence between the translational and torsional responses. As a result of the coupled lateral-torsional response, the induced lateral and torsional forces acting on the asymmetric buildings can, in combination, exceed design values to an extent which would result in wide-spread damage or failure of buildings. The effects of coupled lateral-torsional response have long been observed dur-

ing the investigations of the past earthquakes as well as the parametric studies, e.g. those by Housner and Outinen (1958), Bustamante and Rosenblueth (1960), Medearis (1966), Esteva et al. (1969), Kan and Chopra (1981a, 1981b). They have shown that in the buildings with non-coincident centres of mass and resistance, significant coupling may occur between the translational and the torsional displacements of the structure even when the earthquake excitation is in the form of a uniform rigid base translation. Chandler (1986) found the torsional coupling as a main cause of the damage in the buildings. He reported that 15 percent of the cases of severe damage or collapse of buildings in Mexico City were caused by the pronounced asymmetry in stiffness during Mexico Earthquake, 1985.

Torsional response may also be caused in case of the uncoupled structures if the earthquake input motion at various points underneath the building foundation is not in phase. This effect has been studied by many investigators (e.g. Shibusawa et al. (1969), Newmark (1969), Hart et al. (1975), Tso (1975), Luco (1976), Tso and Hsu (1978), Lin (1989), Gupta and Trifunac (1987a, 1990b)). For the purpose of this study, it will be assumed that the earthquake input motion is identical at all points beneath the structure.

The linear earthquake analysis of rigid based, torsionally coupled buildings has been parametrically studied by Tsienias and Hutchinson (1981, 1982a), Kan and Chopra (1977a), Tso and Dempsey (1980), Dempsey and Irvine (1979) by utilizing the idealized spectral acceleration curves i.e. flat, hyperbolic and flat-hyperbolic. However, the idealization of a spectrum curve in these studies has made the results unsuitable for drawing general conclusions on coupling effects in the asymmetric buildings. For arbitrary-shaped smooth spectra, these studies

were shown to lead to 'too approximate' results by Hejal and Chopra (1989a).

A number of analytical techniques have been formulated for analysing the torsionally coupled buildings and to study the effects of torsional coupling on the earthquake building response. The work of several investigators (e.g., Bustamante and Rosenblueth (1960), Kan and Chopra (1977b), Gluck et al. (1979), Wittrick and Horsington (1979), Tsienias and Hutchinson (1982a), Hejal and Chopra (1989a)) has shown that the dynamic response of an asymmetric multi-storeyed building can be obtained by an analysis of the corresponding symmetric structure (with uncoupled translational and torsional vibration modes), together with that of a single-storey torsionally coupled system. However, this approach gives reasonable results only for a special class of buildings which satisfy the following restrictions: i) the centres of mass of all the floors and the centres of resistance of all the storeys lie on two vertical straight lines, and the radii of gyration for all the floors are same, ii) the ratios of the three stiffness quantities, i.e. translational stiffnesses in X and Y-direction, K_{xI} and K_{yI} , and torsional stiffness $K_{\theta I}$, for any storey are independent of the storey level. Although these studies have provided valuable information on the response of asymmetric buildings, their results can't be generalized to arrive at the widely acceptable conclusions.

Kan and Chopra (1977c) and Tsienias and Hutchinson (1982b) applied the perturbation analysis for the determination of approximate natural frequencies and mode shapes of the torsionally coupled buildings. But the error due to the perturbation analysis was considerable in case of large static eccentricities or closely spaced frequencies of the corresponding torsionally uncoupled systems. Dempsey and Tso (1982), Chandler and Hutchinson (1986, 1987) have used the

time-history approach for the study of seismic torsional effects in asymmetrical buildings. Other investigators who also studied the torsional response of asymmetric buildings, include Penzien (1969), Gibson et al. (1972), Douglas and Trabert (1973), Keintzel (1973), Rutenberg et al. (1978), Lam and Scavuzzo (1981), Tso (1983), Wu and Leyendecker (1984), Hucklebridge and Lei (1986), Hejal and Chopra (1989b), and Maher et al. (1991).

Among most of the previous studies of torsionally coupled single-storey and multistoreyed buildings, various simple response spectrum techniques have been widely used to obtain the deterministic estimates of structural response. However, the uncertainties involved in defining the earthquake motions can properly be accounted for by using a method of seismic response analysis based on the stochastic model of ground motion. In case of linear structures, many investigators (e.g., Tajimi (1960), Caughey and Gray (1963), Hammond (1968), Rosenblueth and Elorduy (1969), Ruiz and Penzien (1971), Udwadia and Trifunac (1974), Singh and Chu (1976), Kaul (1978), Gasparini (1979), Hadjian (1981), Kiureghian (1980, 1981), Amini and Trifunac (1981, 1985), Kung and Pecknold (1984), Rady and Hutchinson (1988), Hutchinson et al. (1991), Gupta and Trifunac (1987b, 1988, 1990a,c, 1992)) have recognized this and described the structural response from a stochastic viewpoint. Only a few of these studies were made for the torsionally coupled models.

Kung and Pecknold (1984) assumed the ground motion to be as a white noise input. Rady and Hutchinson (1988) used a more realistic ground acceleration power spectrum to study the response of torsionally coupled structures. However, due to the limitation of these studies to a single storey model, their re-

sults can't be generalized to the multistoreyed buildings. Hutchinson et al. (1991) have used the stochastic approach to study the effects of vertical mass and stiffness distribution for a special class of multistoreyed buildings. Thus, there exists a need for a more comprehensive investigation of the torsionally coupled multi-storeyed buildings from a stochastic viewpoint.

It is to be noted that the previous studies on torsionally coupled buildings can provide only the amplitude of the largest response peak. However, the design of structures with varying degrees of importance may require response estimates based on different probabilities of exceedance, and the knowledge of higher order peaks is necessary for better understanding of the progressing damage, as the structure is subjected to successive excursions beyond the design level. Thus, it is desirable to develop a response spectrum technique which can estimate the various orders of peaks for a given probability of exceedance. This should also be generalized enough to work for earthquake excitations with varying characteristics, and for the structures with significant correlation between different modes of vibration. Many studies (Amini and Trifunac (1981, 1985), Gupta and Trifunac (1987b, 1988, 1990a,c, 1992)) have already considered this using a torsionally uncoupled model. Thus, it would seem proper to extend these ideas to the fresh investigation of the behaviour of torsionally coupled buildings.

The concept of dynamic eccentricity and associated dynamic amplification of eccentricity for incorporating the torsional effects in buildings has been adopted in major building codes on the basis of several studies by Rosenblueth (1979), Tso and Dempsey (1980), Tso and Meng (1982), Tsienias and Hutchinson (1982a), Hutchinson and Chandler (1986), Chandler and Hutchinson

son (1986, 1988). These studies have primarily used the single-storey models with the eccentricities between the centres of mass and resistance at floor level, being perpendicular to the direction of earthquake excitation. In their studies, they have pointed out that the results of single-storey buildings could be used in case of a special class of multistoreyed buildings. These studies have, however, been ambiguous on the application part of their recommendations.

The objective of the work presented here is to evaluate the stochastic response of linear torsionally coupled buildings due to the single component of ground excitation. An approach, based on the stochastic model of earthquake excitation and the ideas of order statistics, is developed here which can provide amplitudes of all the significant peaks of the response with desired level of confidence while accounting for the interaction between various modes. The concept of equivalent single-storey model used to estimate the dynamic amplification of eccentricity in the torsionally coupled multistorey buildings, has been illustrated through a detailed parametric study of single and multistoreyed example buildings and through various types of earthquake excitations.

1.2 Organization

This work has been presented in four chapters following this chapter.

In Chapter II, the formulation of the stochastic approach has been presented for estimating the response peaks of fixed-base torsionally coupled multistoreyed buildings subjected to single component of the seismic excitation. A lumped mass model of the building, having three degrees of freedom at each floor, has been considered for this purpose. By taking the examples of two buildings

and three different seismic excitations, the proposed approach has been illustrated.

Chapter III is regarding the study of dynamic amplification of eccentricity in unsymmetrical buildings by using the stochastic approach developed in Chapter II. It has been shown how a single-storey model can be used to approximate the dependence of dynamic eccentricity on static eccentricity in case of a typical floor of a multistorey building.

A brief summary and conclusions of this study are presented in Chapter IV.

CHAPTER II

FORMULATION OF STOCHASTIC APPROACH FOR TORSIONALLY COUPLED BUILDINGS

2.1 Brief Review

The statistical distribution of peak amplitudes in a stationary random process has been studied in detail by Rice (1944, 1945) and Cartwright and Longuet-Higgins (1956). Gupta and Trifunac (1988) have used their results to derive the general distribution functions for the various orders of peaks by assuming that the peaks are statistically independent and identically distributed. Those have been further extended for estimating the stochastic response of symmetric multistoreyed buildings which are subjected to translational and rotational components of earthquake excitations (Gupta and Trifunac (1987a,b, 1988, 1990a,c, 1992)). For these applications, a torsionally uncoupled, simple lumped mass model has been considered. Some of the relevant features of the above work are as follows.

Let the random function $f(t)$ e.g. the response of a structure to an earthquake excitation be represented by the sum of an infinite number of sine waves as

$$f(t) = \sum_n c_n \cos(\omega_n t + \phi_n), \quad (2.1.1)$$

where ω_n are the circular frequencies, ϕ_n are the random, uniformly distributed phases, and c_n are the amplitudes such that

$$\sum_{\omega_n=\omega}^{\omega+d\omega} \frac{1}{2} c_n^2 = E(\omega) d\omega. \quad (2.1.2)$$

Here, $E(\omega)$ is the energy spectrum of $f(t)$. Energy spectrum, $E(\omega)$ has been related to the Fourier spectrum, $F(\omega)$ of the function $f(t)$ by (Udwadia and Trifunac (1974), Mohraz and Elghadamsi (1989))

$$E(\omega) = \frac{1}{\pi T} |F(\omega)|^2, \quad (2.1.3)$$

where, T is the total duration of the response.

If all the N peaks of a random (response) function $f(t)$ are assumed to be statistically independent and identically distributed, the n^{th} order peak (in decreasing order of magnitude) with $n \leq N$ is distributed in accordance with the probability distribution function,

$$F_{(n)}(\eta) = \sum_{i=n}^N \binom{N}{i} (P(\eta))^i (1 - P(\eta))^{N-i}, \quad (2.1.4)$$

η being the height of the peak normalized by a_{rms} , the root mean square (r.m.s.) amplitude of $f(t)$, $P(\eta)$ is the probability distribution function of the heights of maxima and it can be expressed as (Cartwright and Longuet-Higgins (1956))

$$P(\eta) = \frac{1}{\sqrt{2\pi}} \left[\int_{\eta/\varepsilon}^{\infty} e^{-x^2/2} dx + (1 - \varepsilon^2)^{1/2} e^{-\eta^2/2} \int_{-\infty}^{\eta(1-\varepsilon^2)^{1/2}/\varepsilon} e^{-x^2/2} dx \right], \quad (2.1.5)$$

where, ε is a measure of the r.m.s. width of the energy spectrum $E(\omega)$. The parameters a_{rms} and ε have been defined in terms of the moments m_n , $n = 0, 2, 4$ of energy spectrum $E(\omega)$ as

$$a_{rms} = \sqrt{m_0} \quad (2.1.6)$$

and

$$\varepsilon = \left[1 - \frac{m_2^2}{m_0 m_4} \right]^{1/2}, \quad (2.1.7)$$

with

$$m_n = \int_0^\infty \omega^n E(\omega) d\omega. \quad (2.1.8)$$

The total number of peaks in $f(t)$ is

$$N = \frac{T}{2\pi} \left(\frac{m_4}{m_2} \right)^{1/2}. \quad (2.1.9)$$

If the r.m.s. value \bar{a} of the peaks of $f(t)$ is used in place of a_{rms} for the calculation of the peak amplitude, $\eta/\sqrt{2}$ is used in place of η as $\bar{a} \simeq \sqrt{2}a_{rms}$, assuming $f(t)$ as a narrow band process (Udwadia and Trifunac (1973)). The expected value of the n^{th} order peak can be found from the expression

$$E[a_{(n)}] = \int_{-\infty}^\infty \eta f_{(n)}(\eta) d\eta, \quad (2.1.10)$$

where, $f_{(n)}(\eta)$ is the probability density function, corresponding to the probability distribution function as in eq. (2.1.4). This can be further written as (Gupta and Trifunac (1988)),

$$f_{(n)}(\eta) = n \binom{N}{n} (P(\eta))^{n-1} (1 - P(\eta))^{N-n} p(\eta), \quad (2.1.11)$$

where, $p(\eta)$ is the probability density function corresponding to $P(\eta)$. The integral in Equation (2.1.10) can be obtained by an approximate approach given by David and Johnson (1954), as also used later by Gupta and Trifunac (1988).

To account for the nonstationary nature of the excitation and the response, Gupta and Trifunac (1987b) have proposed to modify \bar{a} for the i^{th} degree-of-freedom from \bar{a}_i to $(\bar{a}_E)_i$ where

$$(\bar{a}_E)_i = \left[\sum_{j=1}^n (\bar{a}_E)_{ij}^2 \right]^{1/2}. \quad (2.1.12)$$

Here, $(\bar{a}_E)_{ij}$ is the factor which normalizes the maximum value of response function, as calculated from the response spectrum, for the i^{th} degree-of-freedom in the j^{th} mode, to $E[a_{(1)}]_j / \sqrt{2}$. $E[a_{(1)}]_j$ is the expected value of the first order peak response amplitude in the j^{th} mode, in accordance with Eq. (2.1.10). The above procedure can be applied to estimate the stochastic response of any response function in a linear dynamic system from the knowledge of its energy spectrum.

2.2 Equations of Motion

Consider an idealized n -storey unsymmetric building model consisting of rigid floor decks which are supported on massless axially inextensible columns and shear walls, as shown in Fig. 2.1. Following assumptions are made for the present formulation:

- i) The inertia of the i^{th} floor is lumped at the i^{th} floor level by a mass m_i and by a mass moment of inertia, I_i , about the centre of mass of the floor;
- ii) The linear rigidities of the i^{th} storey are provided by the massless columns and shear walls, and are characterized by three constants, the lateral stiffnesses, K_{xi} , K_{yi} along the X and Y-axes, and the torsional stiffness, $K_{\theta i}$ about the vertical Z-axis, passing through the centre of mass;
- iii) The centres of mass of the floors lie on one vertical axis, which coincides with the Z-axis, but the centres of rigidity of the storeys lie on different vertical axes, with static eccentricities, e_{xi} and e_{yi} respectively along the X-axis and Y-axis for the i^{th} storey.

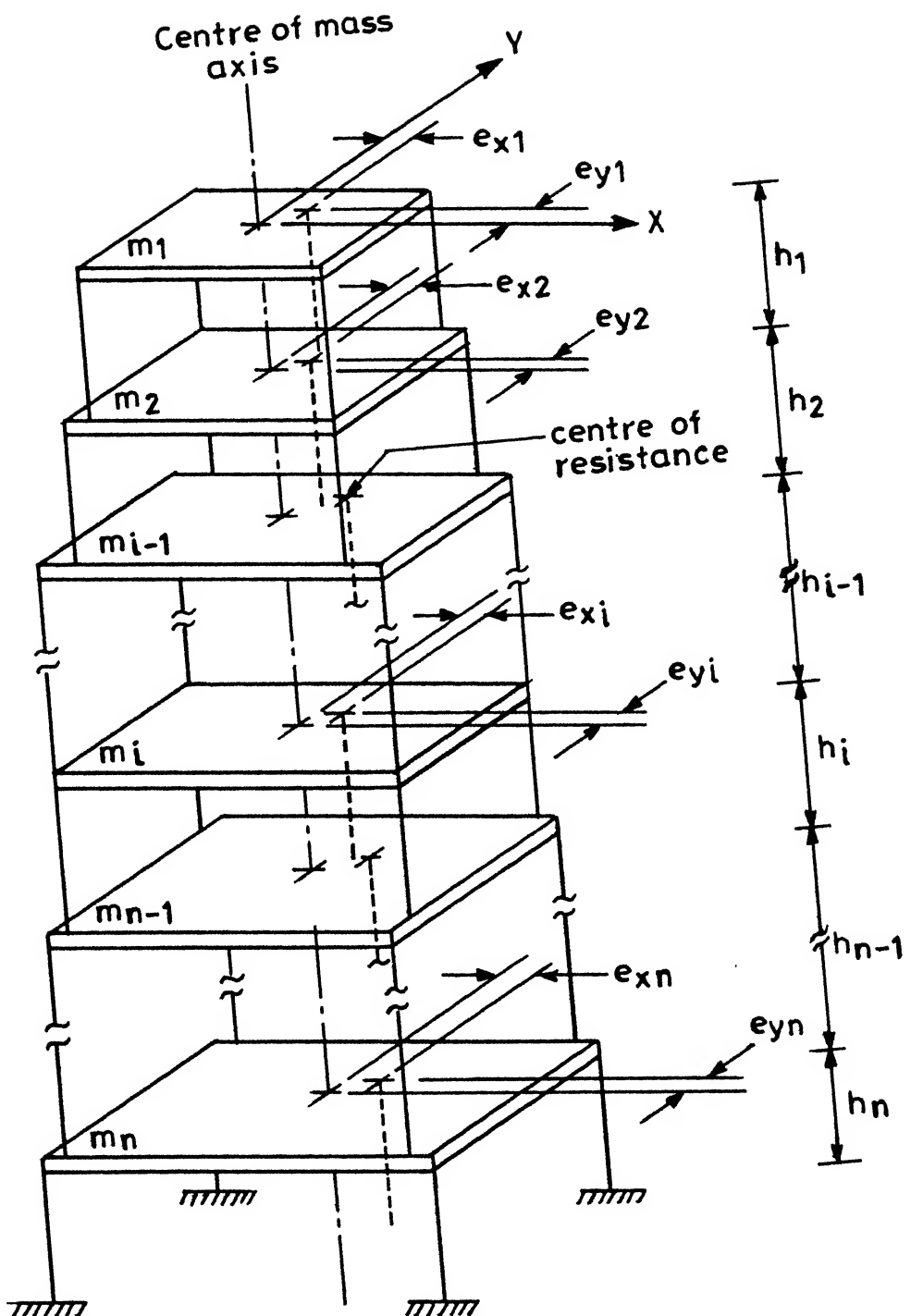


Figure 2.1 Multi-Degree-of-Freedom System for Torsionally Coupled Buildings.

The horizontal reference axes, X and Y of the structure have their origin at the centre of mass as shown in Fig. 2.2. The ground motion is assumed to be in X-direction only. This system has three degrees of freedom for each floor, i.e. X-direction translation (V_X), Y-direction translation (V_Y) and rotation about the centre of mass (V_θ). The equations of motion for the above building model can be expressed as

$$[M]\{\ddot{V}\} + [C]\{\dot{V}\} + [K]\{V\} = -[M]\ddot{Z}_X\{\mathbf{r}\} \quad (2.2.1)$$

in which, $[M]$, $[C]$ and $[K]$ are the inertia, damping and stiffness matrices respectively. $\{V\}$ is the $3n$ -dimensional relative displacement vector and $\ddot{Z}_X(t)$ is the ground acceleration in X-direction. Eq. (2.2.1) can be represented in the matrix form as (Kan and Chopra (1977c)):

$$\begin{bmatrix} [\mathbf{m}] & & \\ & [\mathbf{m}] & \\ & & [\mathbf{m}] \end{bmatrix} \begin{Bmatrix} \ddot{V}_X \\ \ddot{V}_Y \\ \ddot{V}_\theta \end{Bmatrix} + \begin{bmatrix} [\mathbf{C}_X] & [0] & [\mathbf{C}_{X\theta}] \\ [0] & [\mathbf{C}_Y] & [\mathbf{C}_{Y\theta}] \\ [\mathbf{C}_{X\theta}]^T & [\mathbf{C}_{Y\theta}]^T & [\mathbf{C}_\theta] \end{bmatrix} \begin{Bmatrix} \dot{V}_X \\ \dot{V}_Y \\ \dot{V}_\theta \end{Bmatrix} + \\ \begin{bmatrix} [\mathbf{K}_X] & [0] & [\mathbf{K}_{X\theta}] \\ [0] & [\mathbf{K}_Y] & [\mathbf{K}_{Y\theta}] \\ [\mathbf{K}_{X\theta}]^T & [\mathbf{K}_{Y\theta}]^T & [\mathbf{K}_\theta] \end{bmatrix} \begin{Bmatrix} V_X \\ V_Y \\ V_\theta \end{Bmatrix} = -\ddot{Z}_X \begin{bmatrix} [\mathbf{m}] & & \\ & [\mathbf{m}] & \\ & & [\mathbf{m}] \end{bmatrix} \begin{Bmatrix} \{1\} \\ \{0\} \\ \{0\} \end{Bmatrix} \quad (2.2.2)$$

The coefficient matrices in Eq. (2.2.2) can be represented as

$$[\mathbf{m}] = \begin{bmatrix} m_1 & & & & \\ & m_2 & & & \\ & & \ddots & & \\ & & & m_i & \\ & & & & \ddots \\ & & & & & m_n \end{bmatrix}$$

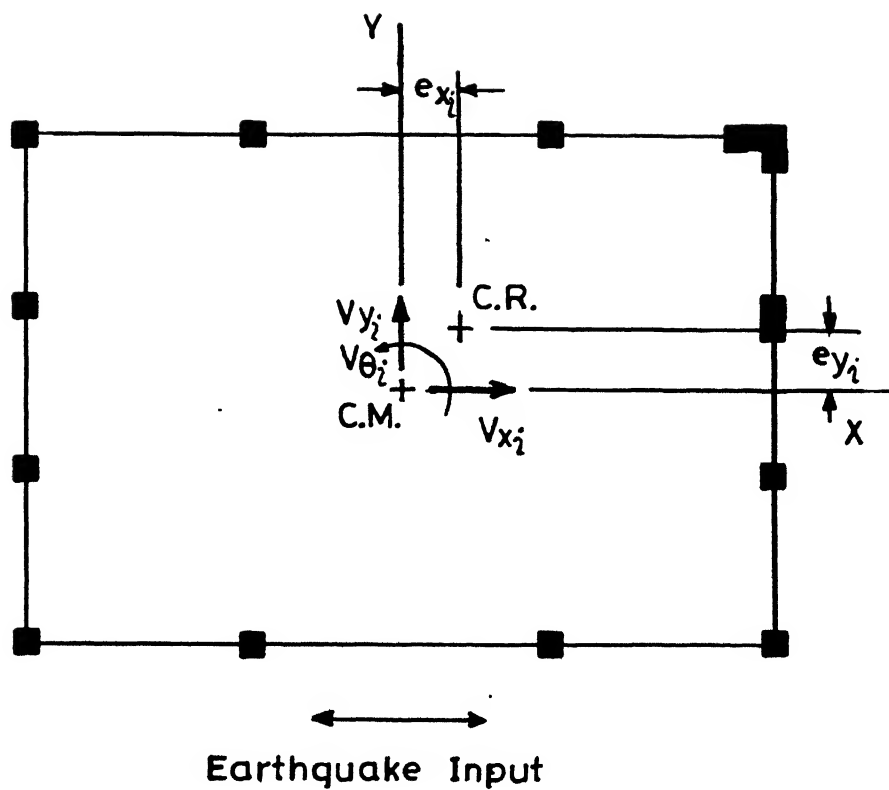


Figure 2.2 *i*-th Floor Level of the Building.

$$\begin{aligned}
 [\mathbf{K}_X] &= \begin{bmatrix} K_{x1} & -K_{x1} & & & & \\ -K_{x1} & (K_{x1} + K_{x2}) & -K_{x2} & & & \\ & -K_{x2} & (K_{x2} + K_{x3}) & \ddots & & \\ & & \ddots & \ddots & -K_{xn-1} & \\ & & & -K_{xn-1} & (K_{xn-1} + K_{xn}) & \end{bmatrix} \\
 [\mathbf{K}_Y] &= \begin{bmatrix} K_{y1} & -K_{y1} & & & & \\ -K_{y1} & (K_{y1} + K_{y2}) & -K_{y2} & & & \\ & -K_{y2} & (K_{y2} + K_{y3}) & \ddots & & \\ & & \ddots & \ddots & -K_{yn-1} & \\ & & & -K_{yn-1} & (K_{yn-1} + K_{yn}) & \end{bmatrix} \\
 [\mathbf{K}_\theta] &= \begin{bmatrix} \left(\frac{1}{r_1}\right)^2 K_{\theta 1} & -\frac{1}{r_1 r_2} K_{\theta 1} & & & & \\ -\frac{1}{r_1 r_2} K_{\theta 1} & \left(\frac{1}{r_2}\right)^2 (K_{\theta 1} + K_{\theta 2}) & -\frac{1}{r_2 r_3} K_{\theta 2} & & & \\ & -\frac{1}{r_2 r_3} K_{\theta 2} & \left(\frac{1}{r_3}\right)^2 (K_{\theta 2} + K_{\theta 3}) & \ddots & & \\ & & \ddots & \ddots & -\frac{1}{r_{n-1} r_n} K_{\theta n-1} & \\ & & & -\frac{1}{r_{n-1} r_n} K_{\theta n-1} & \left(\frac{1}{r_n}\right)^2 (K_{\theta n-1} + K_{\theta n}) & \end{bmatrix} \\
 [\mathbf{K}_{X\theta}] &= - \begin{bmatrix} \frac{1}{r_1} e_{y1} K_{x1} & -\frac{1}{r_2} e_{y1} K_{x1} & & & & \\ -\frac{1}{r_1} e_{y1} K_{x1} & \frac{1}{r_2} (e_{y1} K_{x1} + e_{y2} K_{x2}) & -\frac{1}{r_3} e_{y2} K_{x2} & & & \\ & -\frac{1}{r_2} e_{y2} K_{x2} & \frac{1}{r_3} (e_{y2} K_{x2} + e_{y3} K_{x3}) & \ddots & & \\ & & \ddots & \ddots & -\frac{1}{r_n} e_{yn-1} K_{xn-1} & \\ & & & -\frac{1}{r_{n-1}} e_{yn-1} K_{xn-1} & \frac{1}{r_n} (e_{yn-1} K_{xn-1} + e_{yn} K_{xn}) & \end{bmatrix} \\
 [\mathbf{K}_{Y\theta}] &= - \begin{bmatrix} \frac{1}{r_1} e_{x1} K_{y1} & -\frac{1}{r_2} e_{x1} K_{y1} & & & & \\ -\frac{1}{r_1} e_{x1} K_{y1} & \frac{1}{r_2} (e_{x1} K_{y1} + e_{x2} K_{y2}) & -\frac{1}{r_3} e_{x2} K_{y2} & & & \\ & -\frac{1}{r_2} e_{x2} K_{y2} & \frac{1}{r_3} (e_{x2} K_{y2} + e_{x3} K_{y3}) & \ddots & & \\ & & \ddots & \ddots & -\frac{1}{r_n} e_{xn-1} K_{yn-1} & \\ & & & -\frac{1}{r_{n-1}} e_{xn-1} K_{yn-1} & \frac{1}{r_n} (e_{xn-1} K_{yn-1} + e_{xn} K_{yn}) & \end{bmatrix}
 \end{aligned}$$

where, r_i is the radius of gyration of the i^{th} floor about its centre of mass.

Further, the displacement vectors are

$$V_X = \begin{Bmatrix} V_{x1} \\ V_{x2} \\ \vdots \\ V_{xi} \\ \vdots \\ V_{xn} \end{Bmatrix}; \quad V_Y = \begin{Bmatrix} V_{y1} \\ V_{y2} \\ \vdots \\ V_{yi} \\ \vdots \\ V_{yn} \end{Bmatrix}; \quad V_\theta = \begin{Bmatrix} V_{\theta 1} \\ V_{\theta 2} \\ \vdots \\ V_{\theta i} \\ \vdots \\ V_{\theta n} \end{Bmatrix};$$

where, V_{xi} and V_{yi} respectively are the relative displacements of the i^{th} storey level in X and Y-directions, and $V_{\theta i}$ is its relative rotation in the X-Y plane.

Let $\{\xi\}$ be the normal coordinates such that the displacements $\{V\}$ can be defined by the transformation

$$\{V\} = [\Phi]\{\xi\} , \quad (2.2.3)$$

where, $[\Phi]$ is the modal matrix whose columns are the mode shape vectors, and thus $[\Phi] \equiv [\{\phi^1\} \{\phi^2\} \dots \{\phi^{3n}\}]$. Using the Eq. (2.2.3) in Eq. (2.2.1), the equations of motion can then be written as

$$\{\ddot{\xi}\} + [c]\{\dot{\xi}\} + [\omega^2]\{\xi\} = -\ddot{Z}_X[\Phi]^T[M]\{r\}, \quad (2.2.4)$$

where, it is assumed that the system is classically damped and therefore, $[c]$ is a diagonal matrix having the diagonal term as $2\zeta_i\omega_i$; ζ_i , ω_i respectively being the damping ratio and natural frequency in the i^{th} mode. Further, $[\omega^2]$ is a diagonal matrix with the i^{th} diagonal term as ω_i^2 . Thus, the system response in the j^{th} mode of vibration may be described by

$$\ddot{\xi}_j + 2\zeta_j\omega_j\dot{\xi}_j + \omega_j^2\xi_j = -\ddot{Z}_X\alpha_j, \quad (2.2.5)$$

where, α_j is the modal participation factor, given as

$$\alpha_j = \frac{\{\phi^j\}[M]\{\mathbf{r}\}}{\{\phi^j\}^T[M]\{\phi^j\}} \quad ; \quad j = 1, 2, 3 \dots 3n. \quad (2.2.6)$$

2.3 Energy Spectra for the System Response

The transfer function, $H_j(\omega)$ for the displacement response in the j^{th} mode is obtained from the Eq. (2.2.5) as

$$H_j(\omega) = \frac{1}{(\omega_j^2 - \omega^2 + 2i\zeta_j\omega_j\omega)} \quad . \quad (2.3.1)$$

From this follow the energy spectra for the displacement, shear force, overturning moment and storey torque responses of the system as shown below.

i) Displacement

Using Eq. (2.2.3), the transfer function, $H(\omega)$ for the displacement response of the i^{th} degree-of-freedom $V_i(t)$, can be written as

$$H(\omega) = \sum_{j=1}^{3n} \phi_{ij} \alpha_j H_j(\omega) \quad , \quad (2.3.2)$$

where, ϕ_{ij} is the j^{th} element of the i^{th} mode shape vector, $\{\phi^i\}$. Thus, in frequency domain, the displacement response corresponding to the i^{th} degree-of-freedom becomes

$$\begin{aligned} V_i(\omega) &= H(\omega)Z(\omega) \\ &= \left(\sum_{j=1}^{3n} \phi_{ij} \alpha_j H_j(\omega) \right) Z(\omega) \quad , \end{aligned} \quad (2.3.3)$$

where $Z(\omega)$ is the Fourier transform of the input acceleration time history. Now, on using Eq. (2.1.3), the energy spectrum of the displacement response, $V_i(t)$

becomes

$$\begin{aligned} ED_i(\omega) &= \frac{1}{\pi T} |V_i(\omega)|^2 \\ &= \frac{1}{\pi T} V_i(\omega) V_i^*(\omega) \quad . \end{aligned} \quad (2.3.4)$$

Using Eq. (2.3.3) here gives

$$ED_i(\omega) = \frac{1}{\pi T} |Z(\omega)|^2 \sum_{j=1}^{3n} \sum_{k=1}^{3n} \phi_{ij} \alpha_j \phi_{ik} \alpha_k H_j(\omega) H_k^*(\omega)$$

or,

$$\begin{aligned} ED_i(\omega) &= \frac{1}{\pi T} |Z(\omega)|^2 \sum_{j=1}^{3n} \left[\phi_{ij}^2 \alpha_j^2 |H_j(\omega)|^2 + \right. \\ &\quad \left. \sum_{k=1, k \neq j}^{3n} \phi_{ij} \phi_{ik} \alpha_j \alpha_k \operatorname{Re} \left(H_j(\omega) H_k^*(\omega) \right) \right] \quad . \end{aligned} \quad (2.3.5)$$

Here, the double summation term can be seen to represent the effects of interaction of the j^{th} mode with the other modes of vibration. This can be further simplified by using the partial fractions for $\operatorname{Re} \left(H_j(\omega) H_k^*(\omega) \right)$ (as in Gupta and Trifunac (1990a)) as

$$\begin{aligned} ED_i(\omega) &= \frac{1}{\pi T} |Z(\omega)|^2 \sum_{j=1}^{3n} |H_j(\omega)|^2 \left[\phi_{ij}^2 \alpha_j^2 \right. \\ &\quad \left. + \sum_{k=1, k \neq j}^{3n} \phi_{ij} \phi_{ik} \alpha_j \alpha_k \left\{ C_{jk} + \left(1 - \frac{\omega^2}{\omega_j^2} \right) D_{jk} \right\} \right], \end{aligned} \quad (2.3.6)$$

where, C_{jk} and D_{jk} are the coefficients given in terms of ζ_j , ζ_k and $r = \omega_k / \omega_j$ as,

$$C_{jk} = \frac{1}{B_{jk}} [8\zeta_j(\zeta_j + \zeta_k r) \{(1 - r^2)^2 - 4r(\zeta_j - \zeta_k r)(\zeta_k - \zeta_j r)\}] \quad (2.3.7)$$

$$D_{jk} = \frac{1}{B_{jk}} [2(1 - r^2) \{4r(\zeta_j - \zeta_k r)(\zeta_k - \zeta_j r) - (1 - r^2)^2\}] \quad (2.3.8)$$

and

$$B_{jk} = 8r^2 [(\zeta_j^2 + \zeta_k^2)(1 - r^2)^2 - 2(\zeta_k^2 - \zeta_j^2 r^2)(\zeta_j^2 - \zeta_k^2 r^2)] + (1 - r^2)^4 \quad . \quad (2.3.9)$$

ii) ***Shear Force***

a) **Shear Force in X-direction**

It is possible to write the transfer function $H(\omega)$ for the shear force (in X-direction) i.e. $S_{Xi}(t)$ at the i^{th} floor as

$$H(\omega) = \sum_{j=1}^{3n} \omega_j^2 \alpha_j |H_j(\omega)| \left\{ \sum_{l=1}^i m_l \phi_{lj} \right\} , \quad (2.3.10)$$

and thus the Fourier transform of shear force response, $S_{Xi}(t)$ as

$$S_{Xi}(\omega) = \left[\sum_{j=1}^{3n} \omega_j^2 \alpha_j |H_j(\omega)| \left\{ \sum_{l=1}^i m_l \phi_{lj} \right\} \right] |Z(\omega)| . \quad (2.3.11)$$

Using the Eq. (2.1.3), the energy spectrum for $S_{Xi}(t)$ response can be written as

$$\begin{aligned} ES_{Xi}(\omega) = & \frac{1}{\pi T} |Z(\omega)|^2 \sum_{j=1}^{3n} |H_j(\omega)|^2 \left[\left(\sum_{l=1}^i m_l \phi_{lj} \right)^2 \alpha_j^2 \omega_j^4 \right. \\ & + \sum_{k=1, k \neq j}^{3n} \left(\sum_{l=1}^i m_l \phi_{lj} \right) \left(\sum_{l=1}^i m_l \phi_{lk} \right) \alpha_j \alpha_k \omega_j^2 \omega_k^2 \\ & \left. \left\{ C_{jk} + \left(1 - \frac{\omega^2}{\omega_j^2} \right) D_{jk} \right\} \right]. \end{aligned} \quad (2.3.12)$$

b) **Shear Force in Y-direction**

As in the case of $S_{Xi}(t)$, the energy spectrum for $S_{Yi}(t)$ can be written as

$$\begin{aligned} ES_{Yi}(\omega) = & \frac{1}{\pi T} |Z(\omega)|^2 \sum_{j=1}^{3n} |H_j(\omega)|^2 \left[\left(\sum_{l=1}^i m_l \phi_{(l+n)j} \right)^2 \alpha_j^2 \omega_j^4 \right. \\ & + \sum_{k=1, k \neq j}^{3n} \left(\sum_{l=1}^i m_l \phi_{(l+n)j} \right) \left(\sum_{l=1}^i m_l \phi_{(l+n)k} \right) \alpha_j \alpha_k \omega_j^2 \omega_k^2 \\ & \left. \left\{ C_{jk} + \left(1 - \frac{\omega^2}{\omega_j^2} \right) D_{jk} \right\} \right]. \end{aligned} \quad (2.3.13)$$

iii) Overturning Moment

Similarly as above, the expressions of the energy spectra of overturning moments in X and Y-direction i.e. $EM_{Xi}(\omega)$ and $EM_{Yi}(\omega)$ are obtained as

$$EM_{Xi}(\omega) = \frac{1}{\pi T} |Z(\omega)|^2 \sum_{j=1}^{3n} |H_j(\omega)|^2 \left[\left(\sum_{l=1}^i h_l (m_1 \phi_{1j} + \dots + m_l \phi_{lj}) \right)^2 \alpha_j^2 \omega_j^4 + \sum_{k=1, k \neq j}^{3n} \left(\sum_{l=1}^i h_l (m_1 \phi_{1j} + \dots + m_l \phi_{lj}) \right) \left(\sum_{l=1}^i h_l (m_1 \phi_{1k} + \dots + m_l \phi_{lk}) \right) \alpha_j \alpha_k \omega_j^2 \omega_k^2 \left\{ C_{jk} + \left(1 - \frac{\omega^2}{\omega_j^2} \right) D_{jk} \right\} \right], \quad (2.3.14)$$

and

$$EM_{Yi}(\omega) = \frac{1}{\pi T} |Z(\omega)|^2 \sum_{j=1}^{3n} |H_j(\omega)|^2 \left[\left(\sum_{l=1}^i h_l (m_1 \phi_{(n+1)j} + \dots + m_l \phi_{(n+l)j}) \right)^2 \alpha_j^2 \omega_j^4 + \sum_{k=1, k \neq j}^{3n} \left(\sum_{l=1}^i h_l (m_1 \phi_{(n+1)j} + \dots + m_l \phi_{(n+l)j}) \right) \left(\sum_{l=1}^i h_l (m_1 \phi_{(n+1)k} + \dots + m_l \phi_{(n+l)k}) \right) \alpha_j \alpha_k \omega_j^2 \omega_k^2 \left\{ C_{jk} + \left(1 - \frac{\omega^2}{\omega_j^2} \right) D_{jk} \right\} \right]. \quad (2.3.15)$$

iv) Storey Torque

The energy spectrum of the torque about the centre of mass at the i^{th} floor level, i.e. $ET_i(\omega)$ can be obtained as

$$ET_i(\omega) = \frac{1}{\pi T} |Z(\omega)|^2 \sum_{j=1}^{3n} |H_j(\omega)|^2 \left[\left(\sum_{l=1}^i m_l r_l \phi_{(2n+l)j} \right)^2 \alpha_j^2 \omega_j^4 + \sum_{k=1, k \neq j}^{3n} \left(\sum_{l=1}^i m_l r_l \phi_{(2n+l)j} \right) \left(\sum_{l=1}^i m_l r_l \phi_{(2n+1)k} \right) \alpha_j \alpha_k \omega_j^2 \omega_k^2 \left\{ C_{jk} + \left(1 - \frac{\omega^2}{\omega_j^2} \right) D_{jk} \right\} \right]. \quad (2.3.16)$$

2.4 Nonstationarity in System Response

The above formulation is based on the assumption that the system response functions are stationary functions of time. However, an earthquake excitation is a nonstationary process as it builds up over a small period of time and remains stationary for major part of its duration before decaying. During this, the frequency composition of various waves is also altered in the motion recorded at any site. To account for the nonstationary nature of the excitation and thus that of the response, \bar{a}_i is proposed to be modified to $(\bar{a}_E)_i$ such that the expected value of the largest i.e. 1st order peak in each mode of vibration is same as the response spectrum amplitude in that mode (as in Gupta and Tri-funac (1987)). However, to consider the effects of interaction in the j^{th} mode with the other modes as seen in Eq. (2.3.6), the maximum values of response as obtained from the response spectrum amplitudes are modified to include the additional interaction terms as follows:

a) *Displacement*

$$D_{ij} = SD_j \left(\phi_{ij}^2 \alpha_j^2 + \sum_{k=1, k \neq j}^{3n} \phi_{ij} \phi_{ik} \alpha_j \alpha_k C_{jk} \right)^{\frac{1}{2}}, \quad (2.4.1)$$

b) *Shear Force*

X-direction

$$SX_{ij} = SD_j \left[\left(\sum_{l=1}^i m_l \phi_{lj} \right)^2 \alpha_j^2 \omega_j^4 + \sum_{k=1, k \neq j}^{3n} \left(\sum_{l=1}^i m_l \phi_{lj} \right) \left(\sum_{l=1}^i m_l \phi_{lk} \right) \alpha_j \alpha_k \omega_j^2 \omega_k^2 C_{jk} \right]^{\frac{1}{2}}, \quad (2.4.2)$$

Y-direction

$$SY_{ij} = SD_j \left[\left(\sum_{l=1}^i m_l \phi_{(l+n)j} \right)^2 \alpha_j^2 \omega_j^4 + \sum_{k=1, k \neq j}^{3n} \left(\sum_{l=1}^i m_l \phi_{(l+n)j} \right) \left(\sum_{l=1}^i m_l \phi_{(l+n)k} \right) \alpha_j \alpha_k \omega_j^2 \omega_k^2 C_{jk} \right]^{\frac{1}{2}} \quad (2.4.3)$$

c) *Overturning Moment*X-direction

$$MX_{ij} = SD_j \left[\left(\sum_{l=1}^i h_l (m_1 \phi_{1j} + \dots + m_l \phi_{lj}) \right)^2 \alpha_j^2 \omega_j^4 + \sum_{k=1, k \neq j}^{3n} \left(\sum_{l=1}^i h_l (m_1 \phi_{1j} + \dots + m_l \phi_{lj}) \right) \left(\sum_{l=1}^i h_l (m_1 \phi_{1k} + \dots + m_l \phi_{lk}) \right) \alpha_j \alpha_k \omega_j^2 \omega_k^2 C_{jk} \right]^{\frac{1}{2}} \quad (2.4.4)$$

Y-direction,

$$MY_{ij} = SD_j \left[\left(\sum_{l=1}^i h_l (m_1 \phi_{(n+1)j} + \dots + m_l \phi_{(n+l)j}) \right)^2 \alpha_j^2 \omega_j^4 + \sum_{k=1, k \neq j}^{3n} \left(\sum_{l=1}^i h_l (m_1 \phi_{(n+1)j} + \dots + m_l \phi_{(n+l)j}) \right) \left(\sum_{l=1}^i h_l (m_1 \phi_{(n+1)k} + \dots + m_l \phi_{(n+l)k}) \right) \alpha_j \alpha_k \omega_j^2 \omega_k^2 C_{jk} \right]^{\frac{1}{2}} \quad (2.4.5)$$

d) *Storey Torque*

$$T_{ij} = SD_j \left[\left(\sum_{l=1}^i m_l r_l \phi_{(2n+1)j} \right)^2 \alpha_j^2 \omega_j^4 + \sum_{k=1, k \neq j}^{3n} \left(\sum_{l=1}^i m_l r_l \phi_{(2n+1)j} \right) \left(\sum_{l=1}^i m_l r_l \phi_{(2n+1)k} \right) \alpha_j \alpha_k \omega_j^2 \omega_k^2 C_{jk} \right]^{\frac{1}{2}} \quad (2.4.6)$$

In the above equations, C_{jk} is the same as defined earlier in Eq. (2.3.7) and SD_j is the spectral displacement corresponding to the modal frequency ω_j and damping ratio ζ_j . It may be observed that the interaction terms in these equations do not include the terms involving D_{jk} (see Eq. (2.3.6)). This is so because it has been assumed here that the pseudo spectral velocities (PSV) and spectral velocities (SV) of a given excitation are not very different from each other for the considered values of damping ratios and frequencies.

2.5 Illustration of the Proposed Model

Two types of fixed-base multistoreyed buildings have been considered here for the illustration of the approach as formulated above. The first example building is a 7-storey building having a non-uniform floor dimensions, 26 m x 33 m at the bottom three storeys and 20 m x 25 m for the remaining four at the top. Each storey is of constant height 3.75 m. The translational stiffness in X-direction is different from the translational stiffness in Y-direction at each storey level. The static eccentricities in both the directions are different from floor to floor. Thus, the centres of resistance are not lying on a vertical straight line. The second example building is a 15-storey building with uniform floor dimension of 25 m x 100 m at each floor level. Each storey is of constant height 5.0 m, and floor masses and storey stiffnesses vary linearly from top to the bottom storey. Various properties of these buildings are shown in Table 2.1 and Table 2.2. Further, the critical damping ratio has been assumed equal to 0.05 in all the modes for both the buildings. Torsional stiffnesses of various storeys have been computed by neglecting the contributions of the torsional stiffnesses of various supporting structural elements about their longitudinal axes. The natural frequencies of

Table 2.1 - Properties of First Example Building

Floor level, i	Mass m_i	Radius of gyration, r_i	Stiffnesses			Eccentricities	
			K_{xi}	K_{yi}	$K_{\theta i}$	e_{xi}	e_{yi}
1	$0.80m$	$1.0r$	$2.212k$	$1.392k$	$1.680kr^2$	$0.20r$	$0.26r$
2	$0.80m$	$1.0r$	$2.696k$	$2.179k$	$2.311kr^2$	$0.20r$	$0.26r$
3	$0.80m$	$1.0r$	$3.100k$	$2.697k$	$2.837kr^2$	$0.20r$	$0.26r$
4	$0.80m$	$1.0r$	$3.424k$	$3.112k$	$3.257kr^2$	$0.24r$	$0.26r$
5	$1.15m$	$1.3r$	$4.998k$	$4.792k$	$11.094kr^2$	$0.34r$	$0.50r$
6	$1.15m$	$1.3r$	$5.240k$	$5.083k$	$11.718kr^2$	$0.34r$	$0.50r$
7	$1.15m$	$1.3r$	$5.361k$	$5.229k$	$12.878kr^2$	$0.34r$	$0.50r$

$m = 1 \times 10^6 \text{ kg}$, $k = 1 \times 10^9 \text{ N/m}$, $r = 9.242 \text{ m}$.

Table 2.2 - Properties of Second Example Building

Floor level, <i>i</i>	Mass <i>m_i</i>	Radius of gyration, <i>r_i</i>	Stiffnesses			Eccentricities	
1	0.60 <i>m</i>	1.0 <i>r</i>	0.600 <i>k</i>	0.793 <i>k</i>	1.014 <i>kr</i> ²	0.060 <i>r</i>	0.060 <i>r</i>
2	0.63 <i>m</i>	1.0 <i>r</i>	0.623 <i>k</i>	0.824 <i>k</i>	1.053 <i>kr</i> ²	0.063 <i>r</i>	0.063 <i>r</i>
3	0.66 <i>m</i>	1.0 <i>r</i>	0.652 <i>k</i>	0.863 <i>k</i>	1.102 <i>kr</i> ²	0.066 <i>r</i>	0.066 <i>r</i>
4	0.69 <i>m</i>	1.0 <i>r</i>	0.681 <i>k</i>	0.901 <i>k</i>	1.151 <i>kr</i> ²	0.069 <i>r</i>	0.069 <i>r</i>
5	0.72 <i>m</i>	1.0 <i>r</i>	0.710 <i>k</i>	0.939 <i>k</i>	1.200 <i>kr</i> ²	0.072 <i>r</i>	0.072 <i>r</i>
6	0.74 <i>m</i>	1.0 <i>r</i>	0.739 <i>k</i>	0.978 <i>k</i>	1.249 <i>kr</i> ²	0.075 <i>r</i>	0.075 <i>r</i>
7	0.77 <i>m</i>	1.0 <i>r</i>	0.768 <i>k</i>	1.016 <i>k</i>	1.298 <i>kr</i> ²	0.077 <i>r</i>	0.077 <i>r</i>
8	0.80 <i>m</i>	1.0 <i>r</i>	0.797 <i>k</i>	1.054 <i>k</i>	1.347 <i>kr</i> ²	0.080 <i>r</i>	0.080 <i>r</i>
9	0.83 <i>m</i>	1.0 <i>r</i>	0.826 <i>k</i>	1.093 <i>k</i>	1.396 <i>kr</i> ²	0.083 <i>r</i>	0.083 <i>r</i>
10	0.86 <i>m</i>	1.0 <i>r</i>	0.855 <i>k</i>	1.131 <i>k</i>	1.445 <i>kr</i> ²	0.086 <i>r</i>	0.086 <i>r</i>
11	0.89 <i>m</i>	1.0 <i>r</i>	0.884 <i>k</i>	1.170 <i>k</i>	1.494 <i>kr</i> ²	0.089 <i>r</i>	0.089 <i>r</i>
12	0.91 <i>m</i>	1.0 <i>r</i>	0.913 <i>k</i>	1.208 <i>k</i>	1.543 <i>kr</i> ²	0.092 <i>r</i>	0.092 <i>r</i>
13	0.94 <i>m</i>	1.0 <i>r</i>	0.942 <i>k</i>	1.246 <i>k</i>	1.592 <i>kr</i> ²	0.095 <i>r</i>	0.095 <i>r</i>
14	0.97 <i>m</i>	1.0 <i>r</i>	0.971 <i>k</i>	1.213 <i>k</i>	1.641 <i>kr</i> ²	0.097 <i>r</i>	0.097 <i>r</i>
15	1.00 <i>m</i>	1.0 <i>r</i>	1.000 <i>k</i>	1.323 <i>k</i>	1.690 <i>kr</i> ²	0.100 <i>r</i>	0.100 <i>r</i>

$$m = 0.792 \times 10^6 \text{ kg}, k = 1.971 \times 10^9 \text{ N/m}, r = 29.76 \text{ m.}$$

both example buildings are shown in Table 2.3 and Table 2.4.

Two earthquake excitations have been considered, for the illustration here, with the following characteristics:

1. Recorded motion at El Centro site during the Imperial Valley Earthquake, 1940, S00E component.
2. Synthetically generated motion for Mexico Earthquake, 1985 at Mexico City Site (see Gupta and Trifunac (1990c)).

Accelerograms and the corresponding Fourier spectra for the motions as above have been shown in Figs. 2.3 to 2.6. It can be seen that the first example excitation is of narrow band nature with heavy concentration of energy at the periods close to 2.5 sec, while the second excitation is of broad band nature with the distribution of energy in the broad range of 0.2–5 sec. Further, the relative stiffnesses of these example buildings with respect to the example excitations are such that the different levels of interaction effects will be obtained in the building response. The proposed approach is based on the assumption that the considered random function is stationary. Thus, the value of the total time duration T is not taken as the actual record length, \bar{T} . As T should correspond to the stationary part of the excitation, it has been assumed to correspond to that time interval during which 90% of the total energy arrives after the initial arrival of 5% (see Trifunac and Brady (1975)). Therefore, the value of T for these example excitation has been taken as 24.44 sec and 46.44 sec respectively, instead of $\bar{T} = 53.72$ sec and 80.96 sec.

Table 2.3 - Natural Frequencies of First Example Building

Mode #	ω_n (rad/sec)	Mode #	ω_n (rad/sec)
1	12.49	12	77.27
2	14.63	13	88.52
3	18.87	14	91.23
4	29.21	15	96.62
5	34.99	16	100.39
6	42.74	17	108.54
7	45.81	18	113.41
8	55.81	19	122.41
9	63.11	20	129.43
10	67.53	21	156.98
11	75.27		

Table 2.4 - Natural Frequencies of Second Example Building

Mode #	ω_n (rad/sec)	Mode #	ω_n (rad/sec)	Mode #	ω_n (rad/sec)
1	5.55	16	54.35	31	93.24
2	6.34	17	56.35	32	95.54
3	7.35	18	57.30	33	96.01
4	15.00	19	64.92	34	96.78
5	17.16	20	65.06	35	97.70
6	19.81	21	65.63	36	102.28
7	24.32	22	72.23	37	104.21
8	27.82	23	74.40	38	106.64
9	32.08	24	75.68	39	109.80
10	33.05	25	78.90	40	111.74
11	37.80	26	82.72	41	111.78
12	41.20	27	84.62	42	118.12
13	43.58	28	85.95	43	123.15
14	47.15	29	89.43	44	126.79
15	49.25	30	90.23	45	129.13

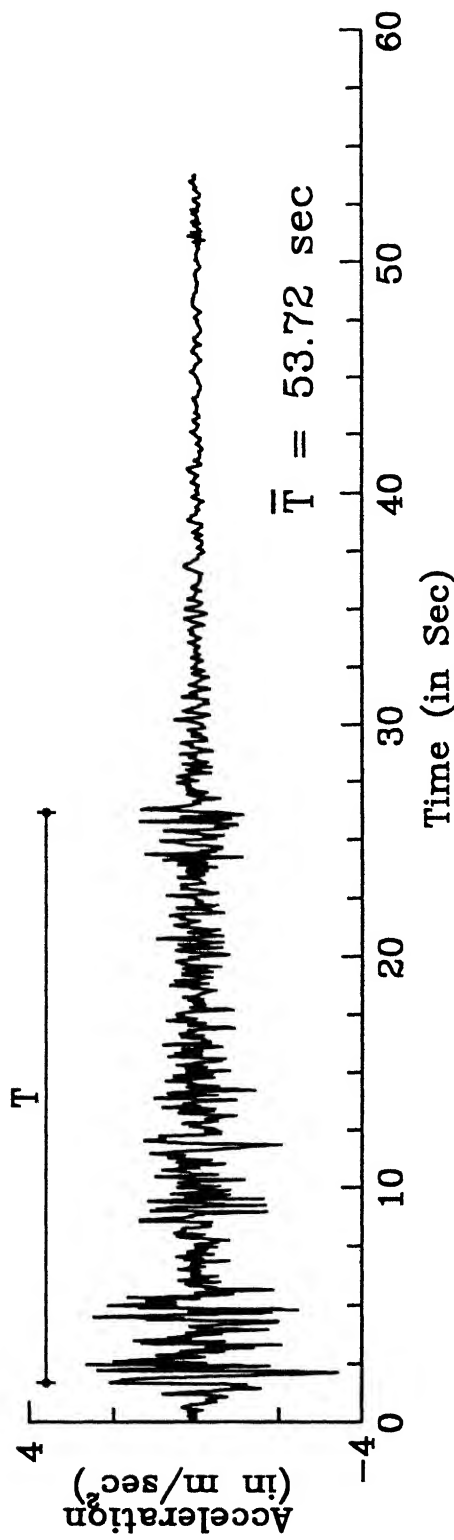
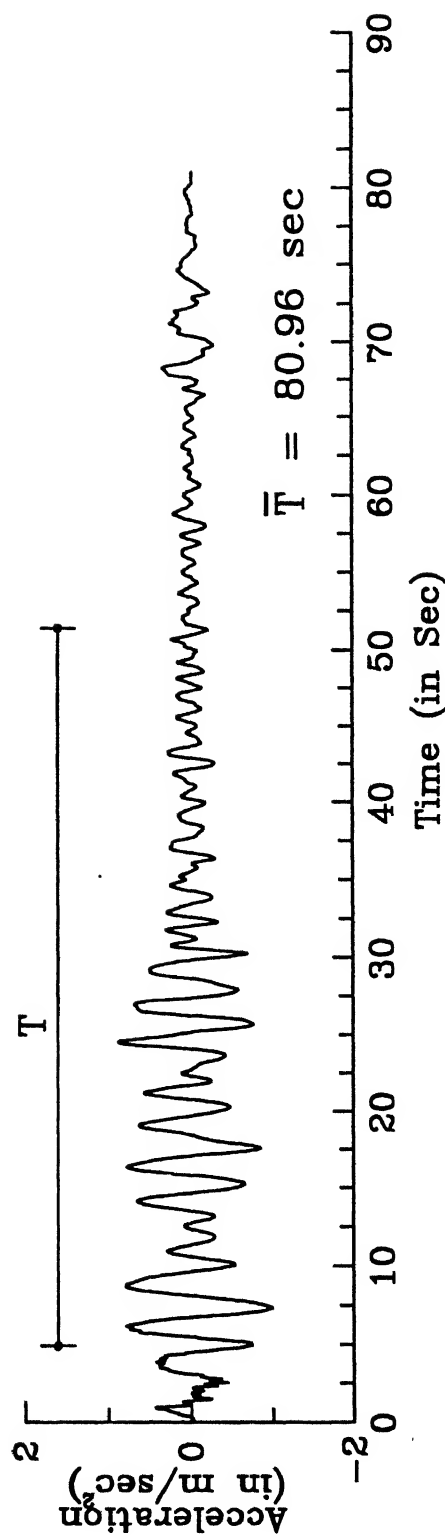


Figure 2.3 Recorded Accelerogram at El Centro Site for S00E component of Imperial Valley Earthquake, 1940.



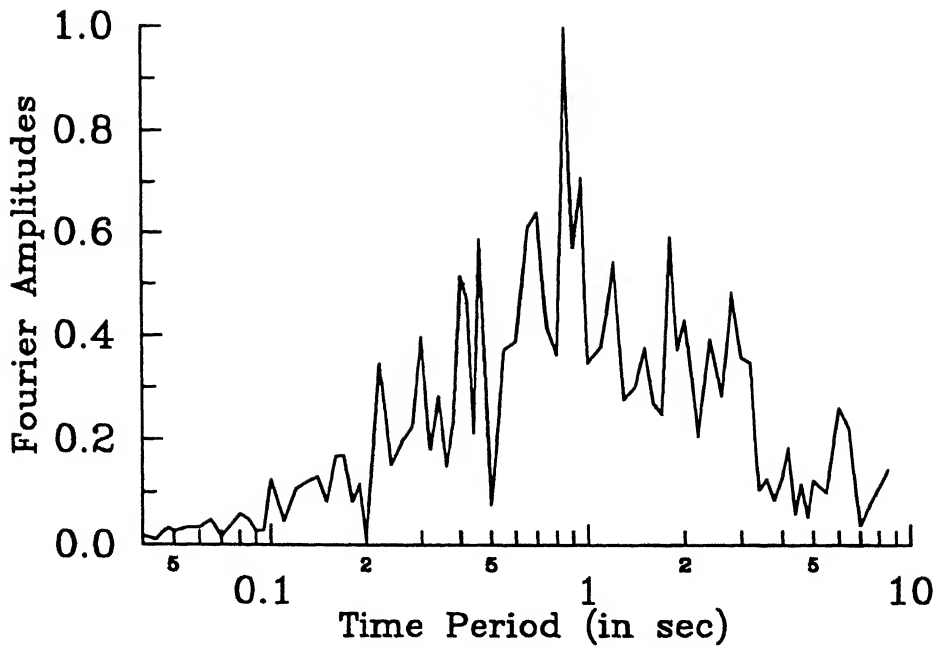


Figure 2.5 Normalized Fourier Spectrum for Imperial Valley Earthquake.

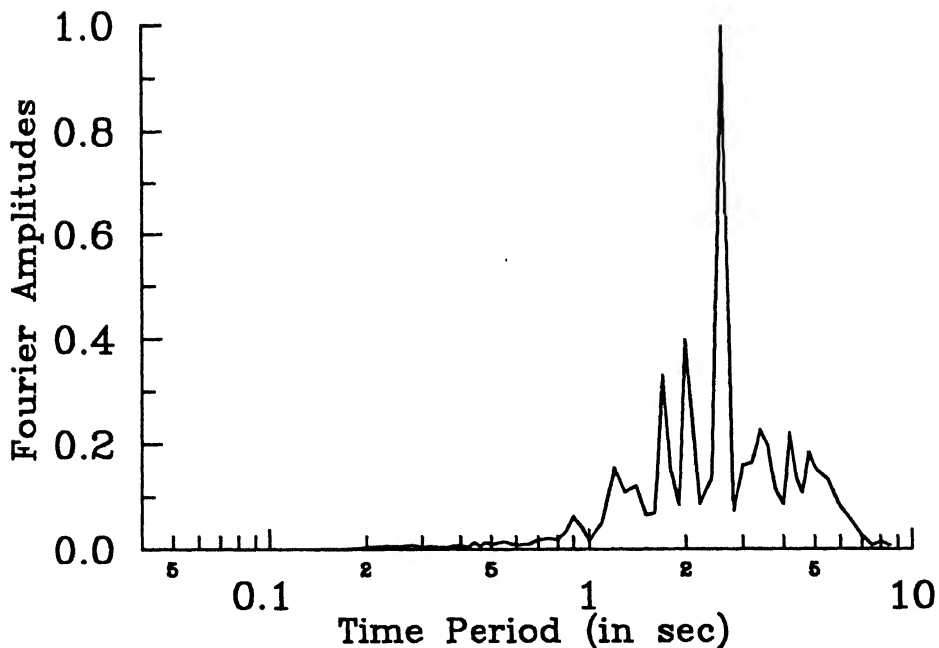


Figure 2.6 Normalized Fourier Spectrum for Mexico Earthquake.

A time domain analysis has been carried out here for the validation of the proposed approach, and the results have been compared by plotting the envelopes of maximum peak displacement, shear force, overturning moment and torque as shown in Figs. 2.7 to 2.18. In each figure, the response values have been normalized with respect to the respective overall maximum response values. It is obvious from these figures that the expected values of the system responses based on the stochastic approach are in close agreement with the time domain analysis results, and that the time domain analysis results are bounded on either side by the 5% and 95% confidence level estimates. Thus it is possible to use the proposed approach for the stochastic response of torsionally coupled structures which are assumed to be subjected to the unidirectional earthquake excitation.

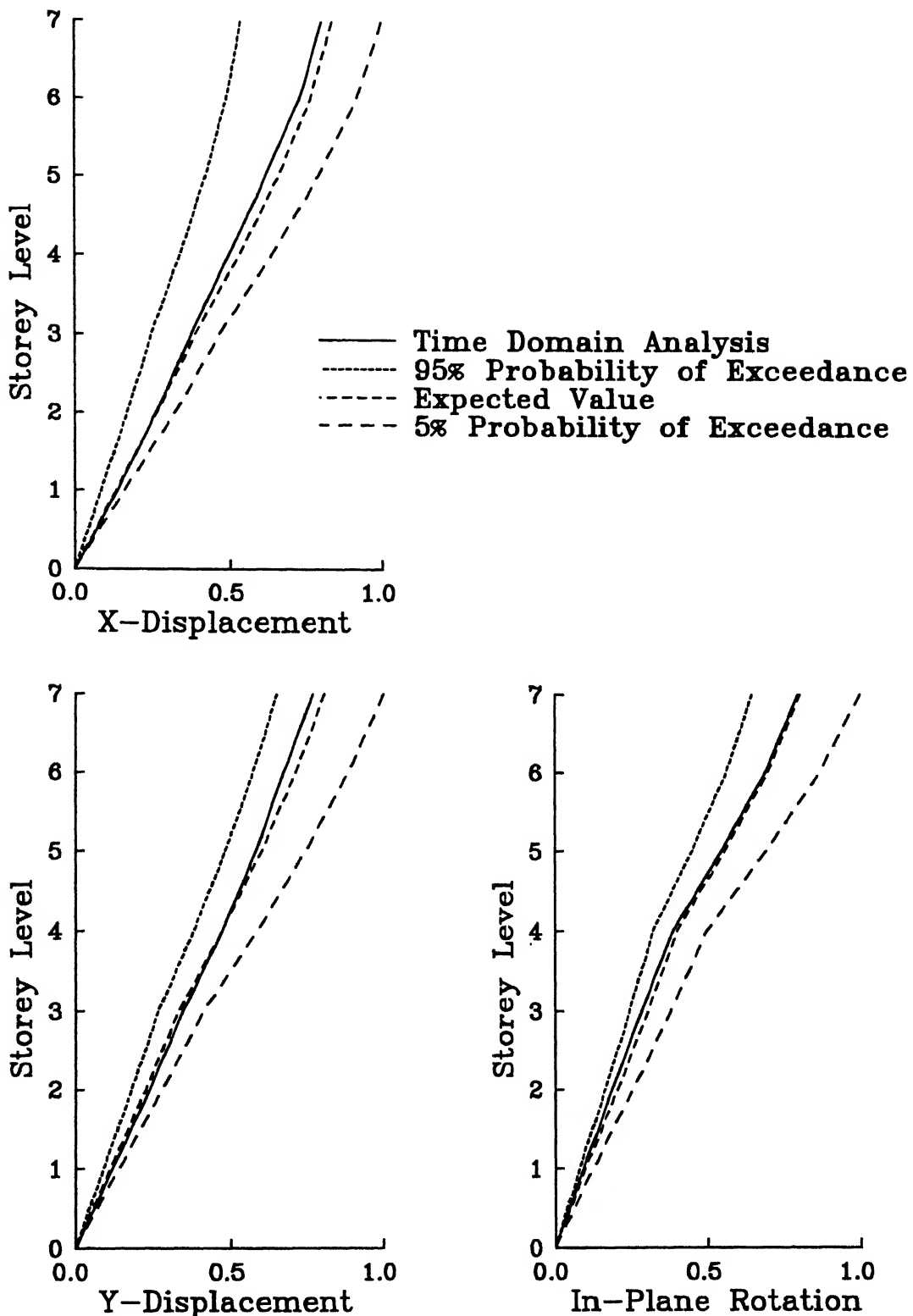


Figure 2.7 Normalized Displacement Responses in First Example Building for Imperial Valley Earthquake.

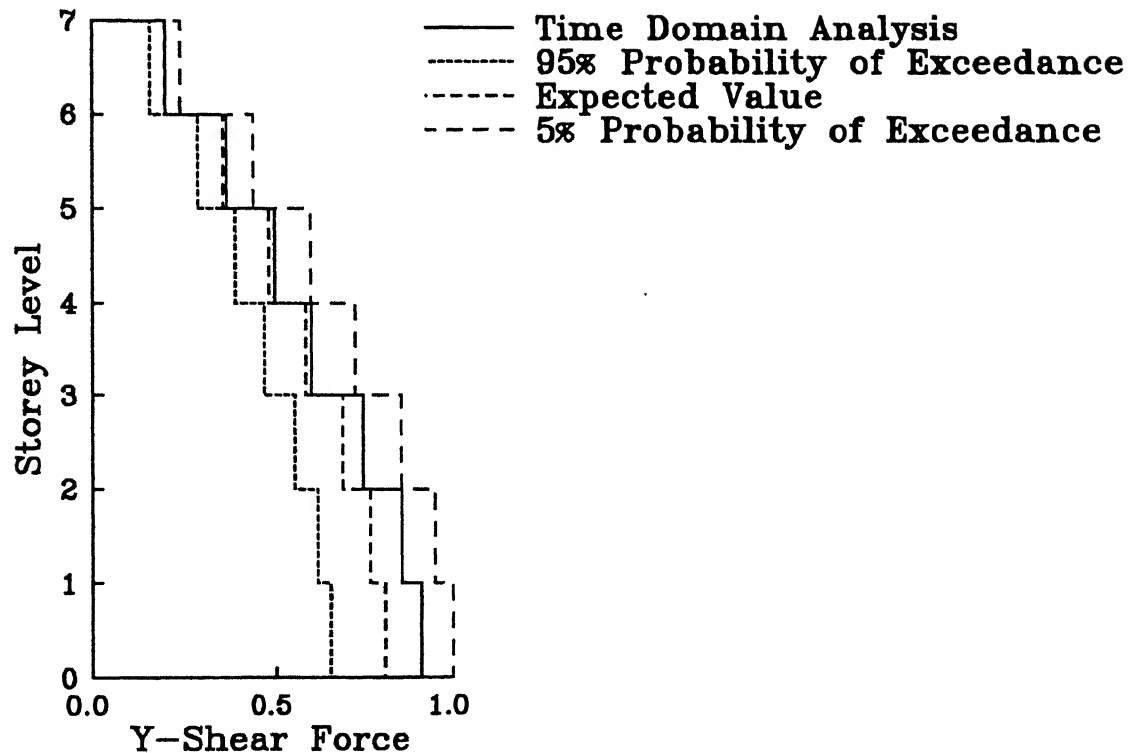
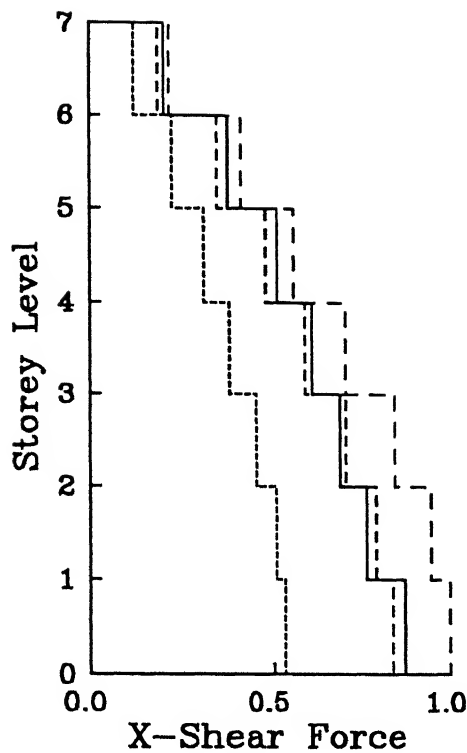


Figure 2.8 Normalized Shear Responses in First Example Building for Imperial Valley Earthquake.

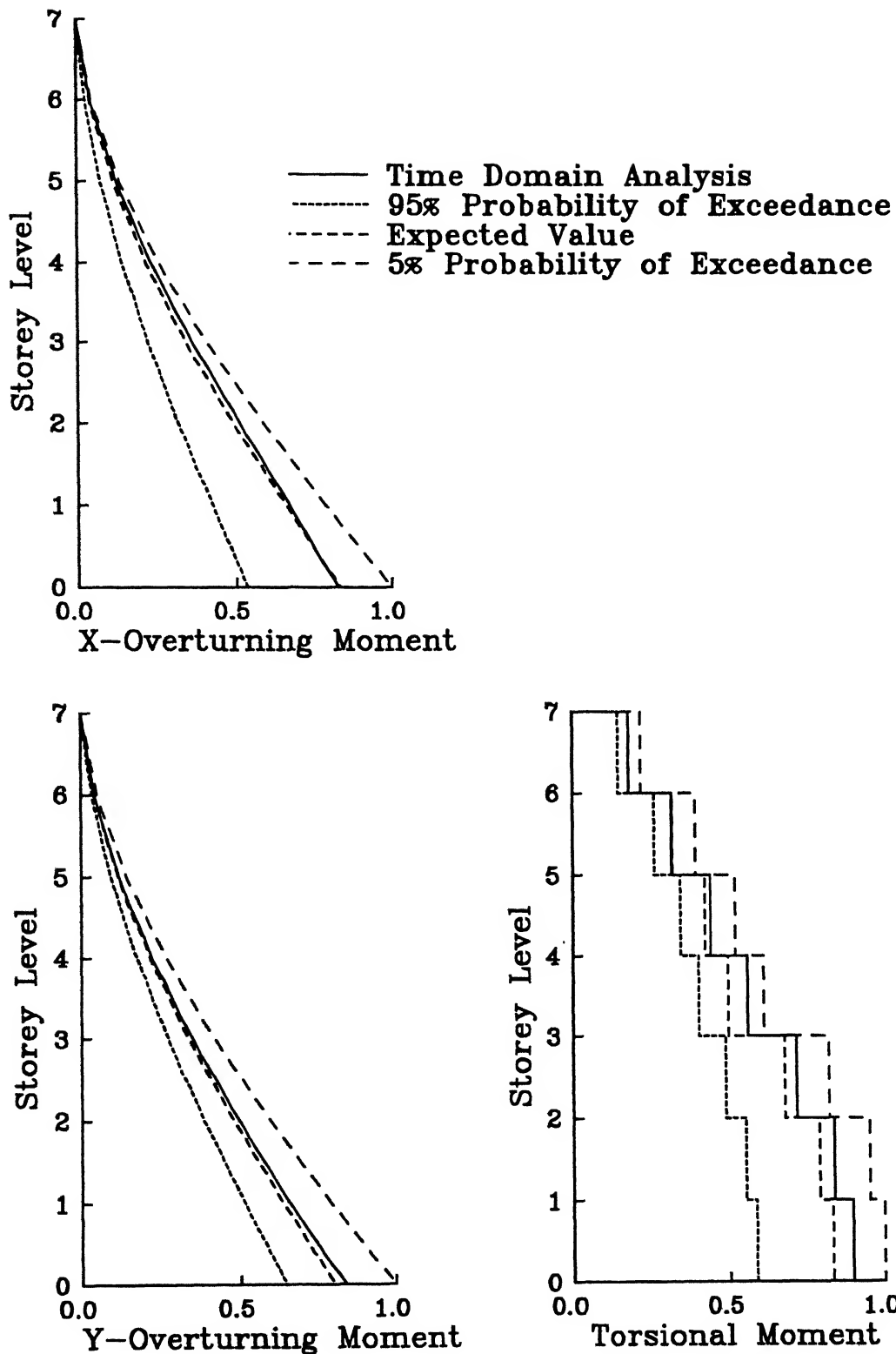


Figure 2.9 Normalized Moment Responses in First Example Building for Imperial Valley Earthquake.

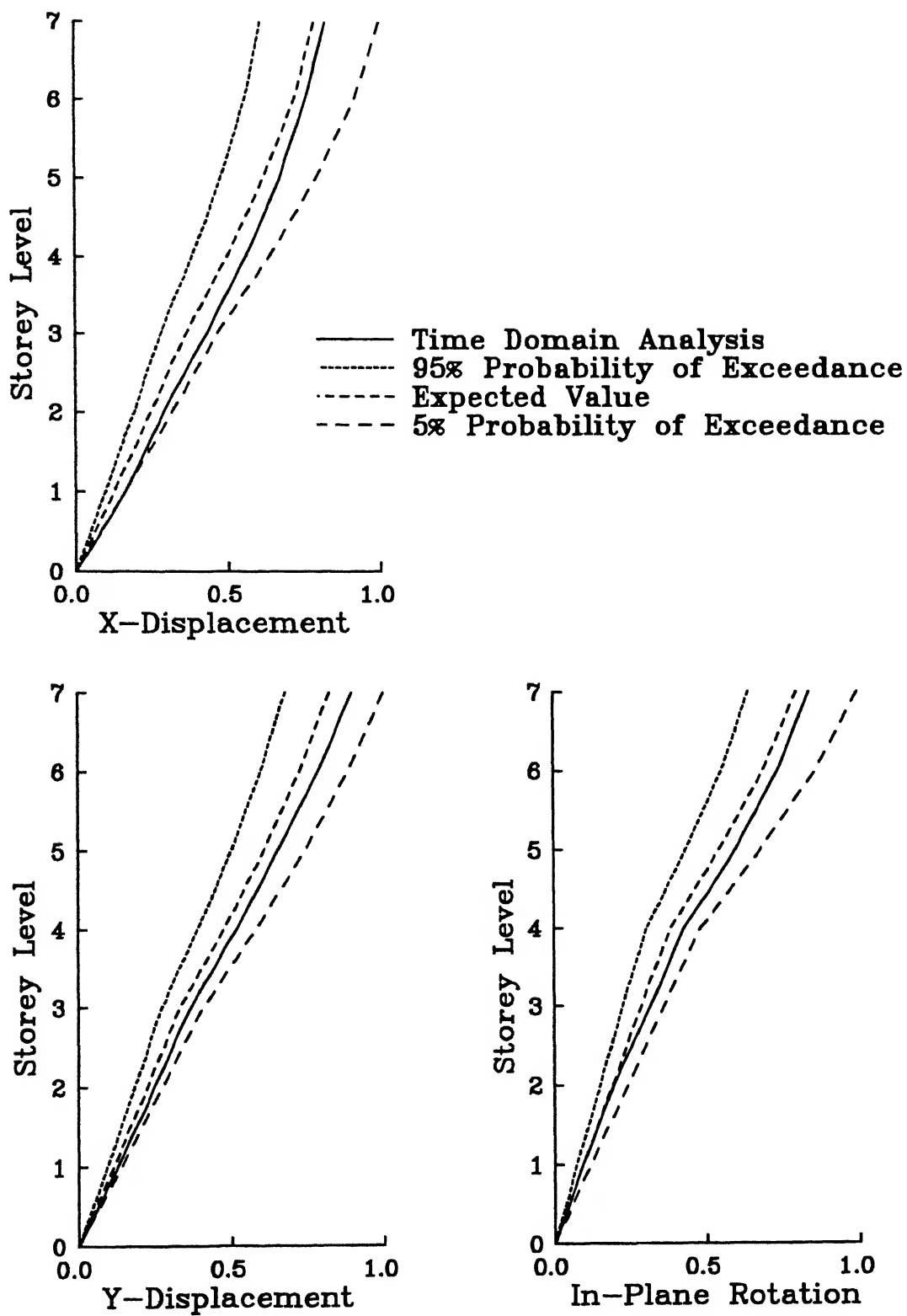


Figure 2.10 Normalized Displacement Responses in First Example Building for Mexico Earthquake.

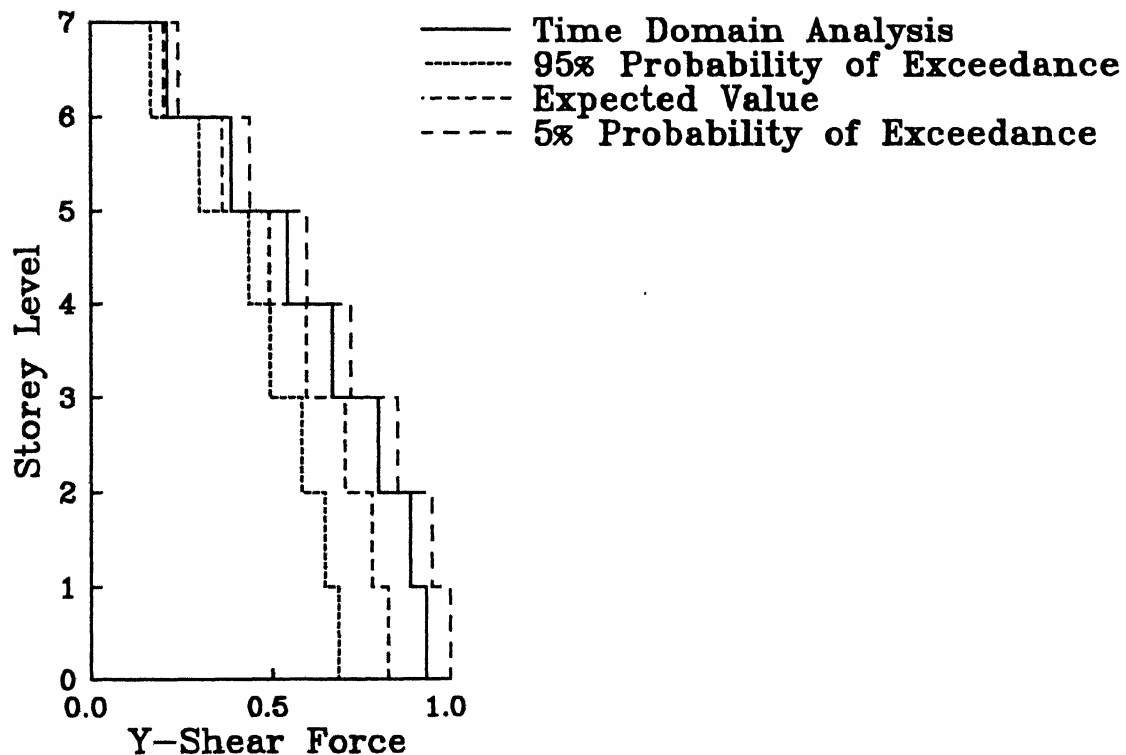
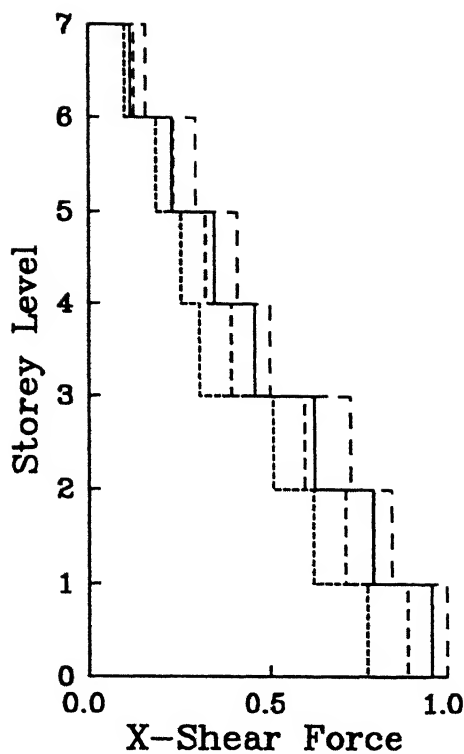


Figure 2.11 Normalized Shear Responses in First Example Building for Mexico Earthquake.

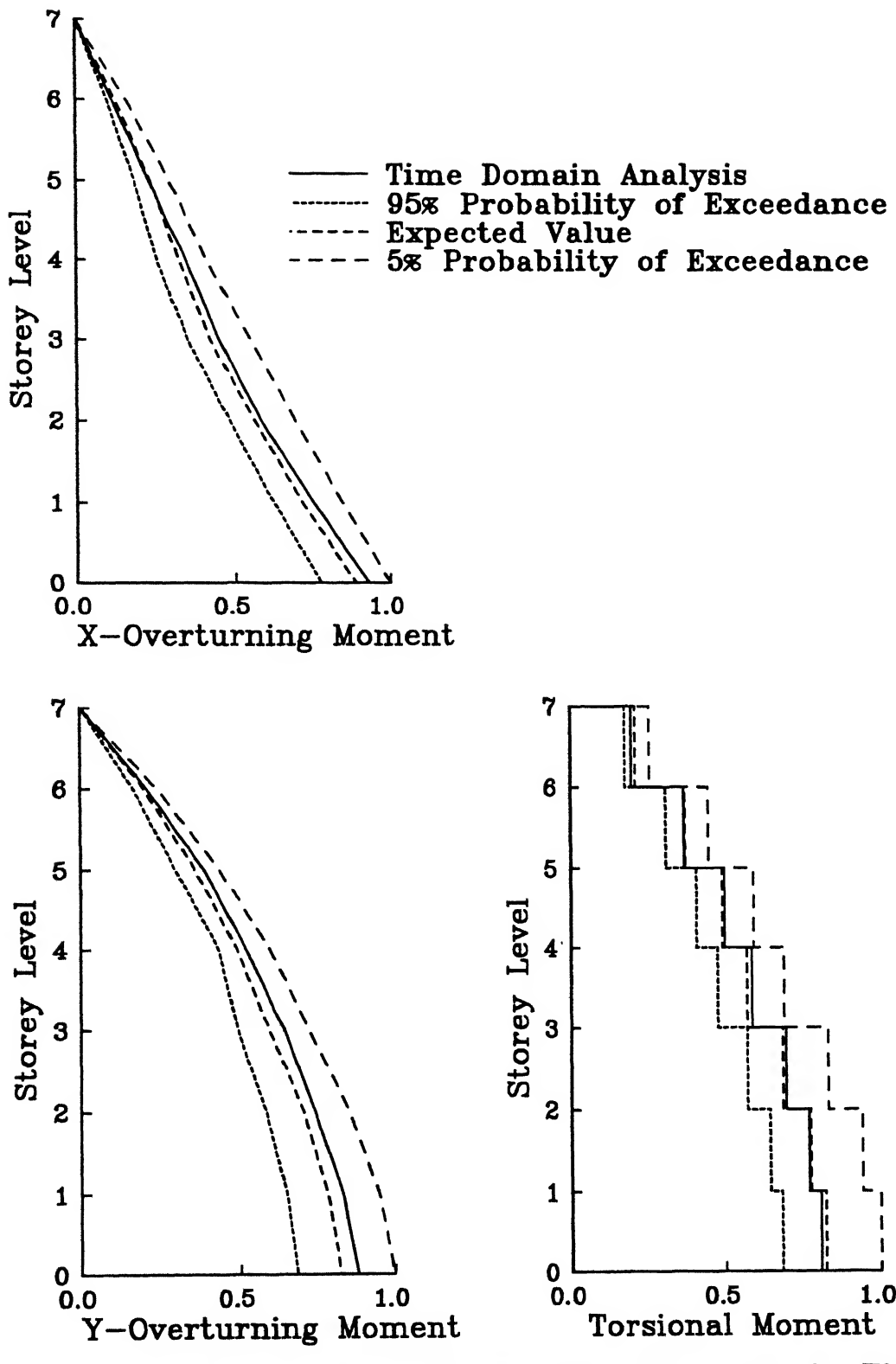


Figure 2.12 Normalized Moment Responses in First Example Building for Mexico Earthquake.

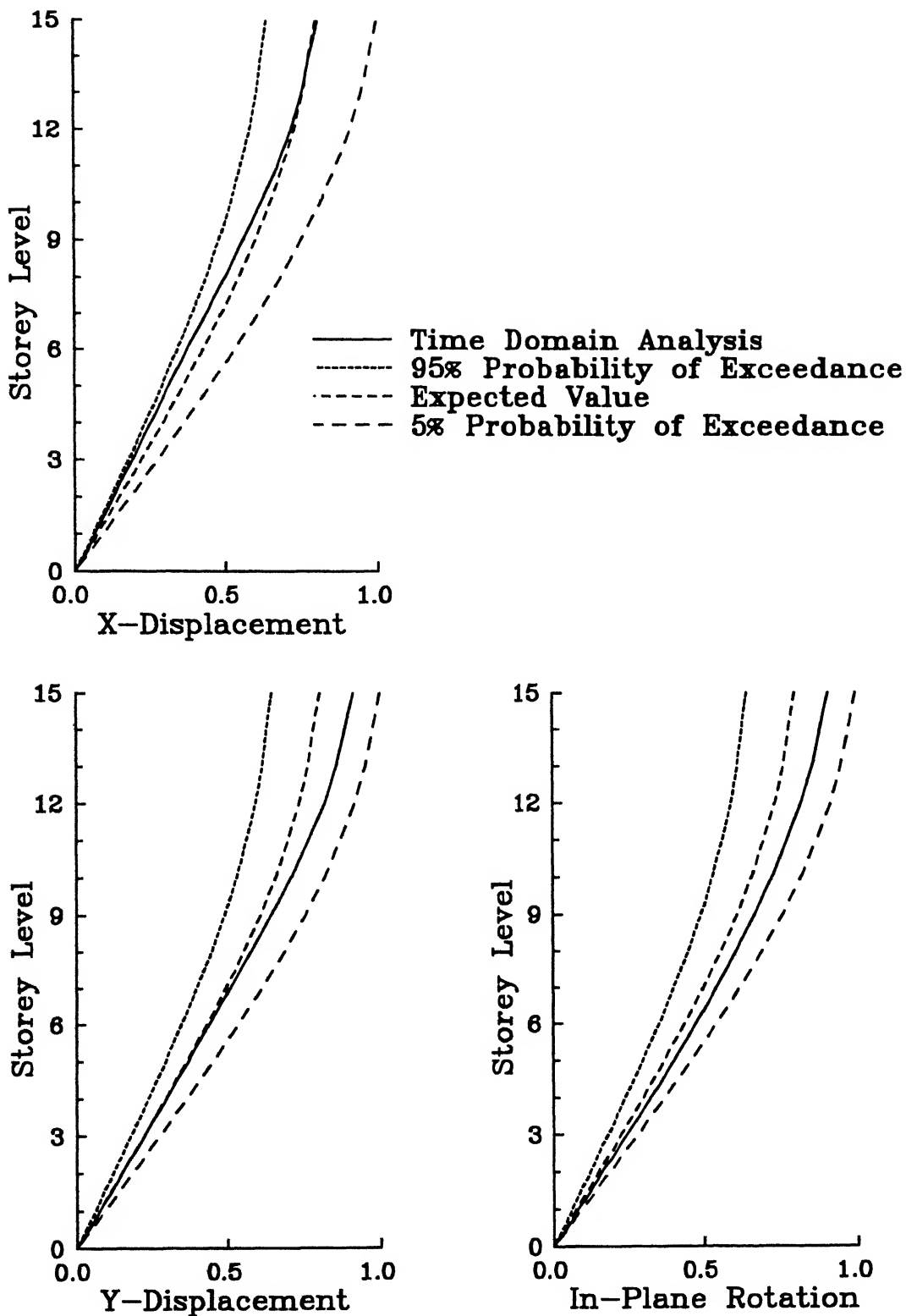


Figure 2.13 Normalized Displacement Responses in Second Example Building for Imperial Valley Earthquake.

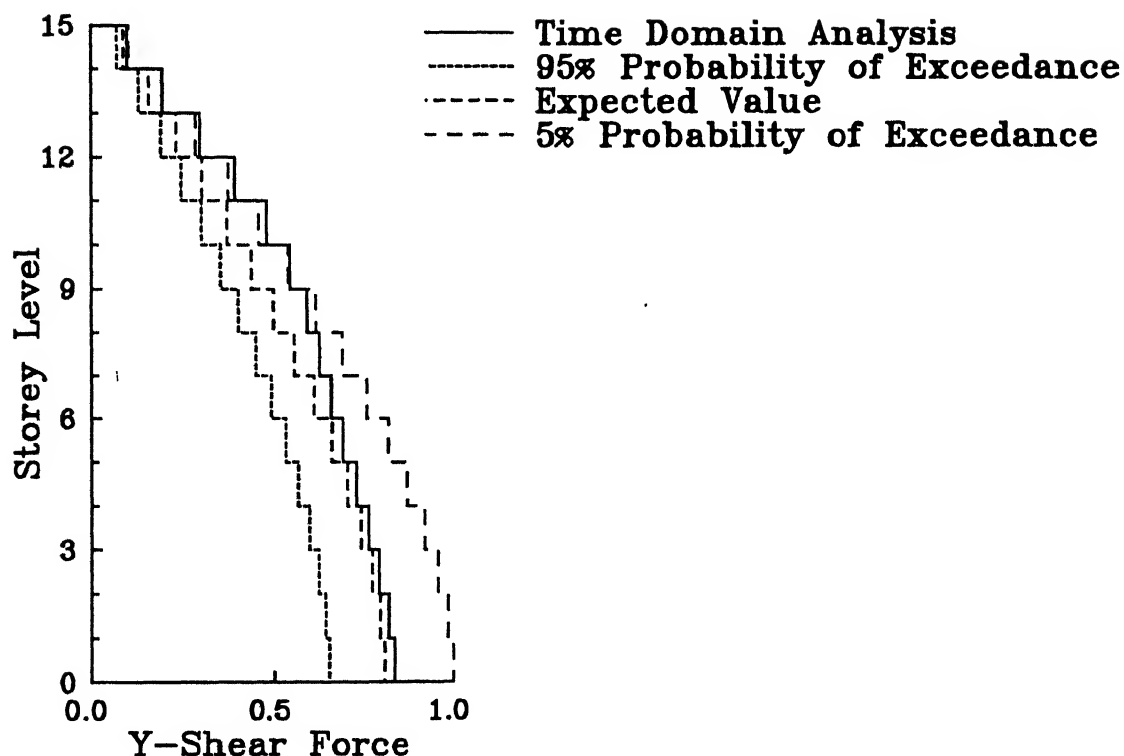
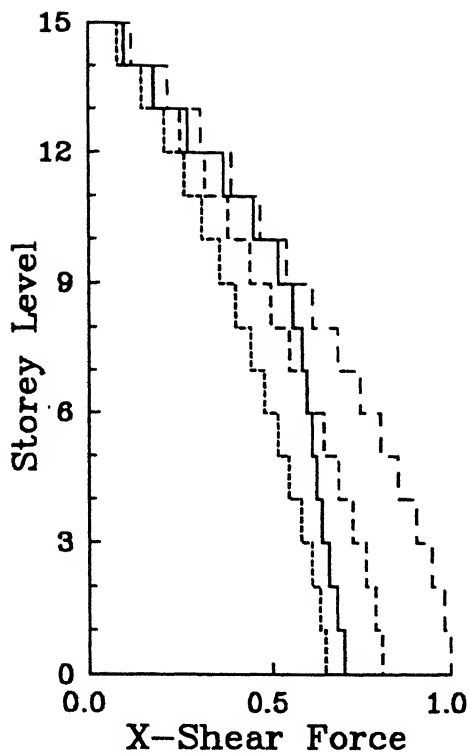


Figure 2.14 Normalized Shear Responses in Second Example Building for Imperial Valley Earthquake.

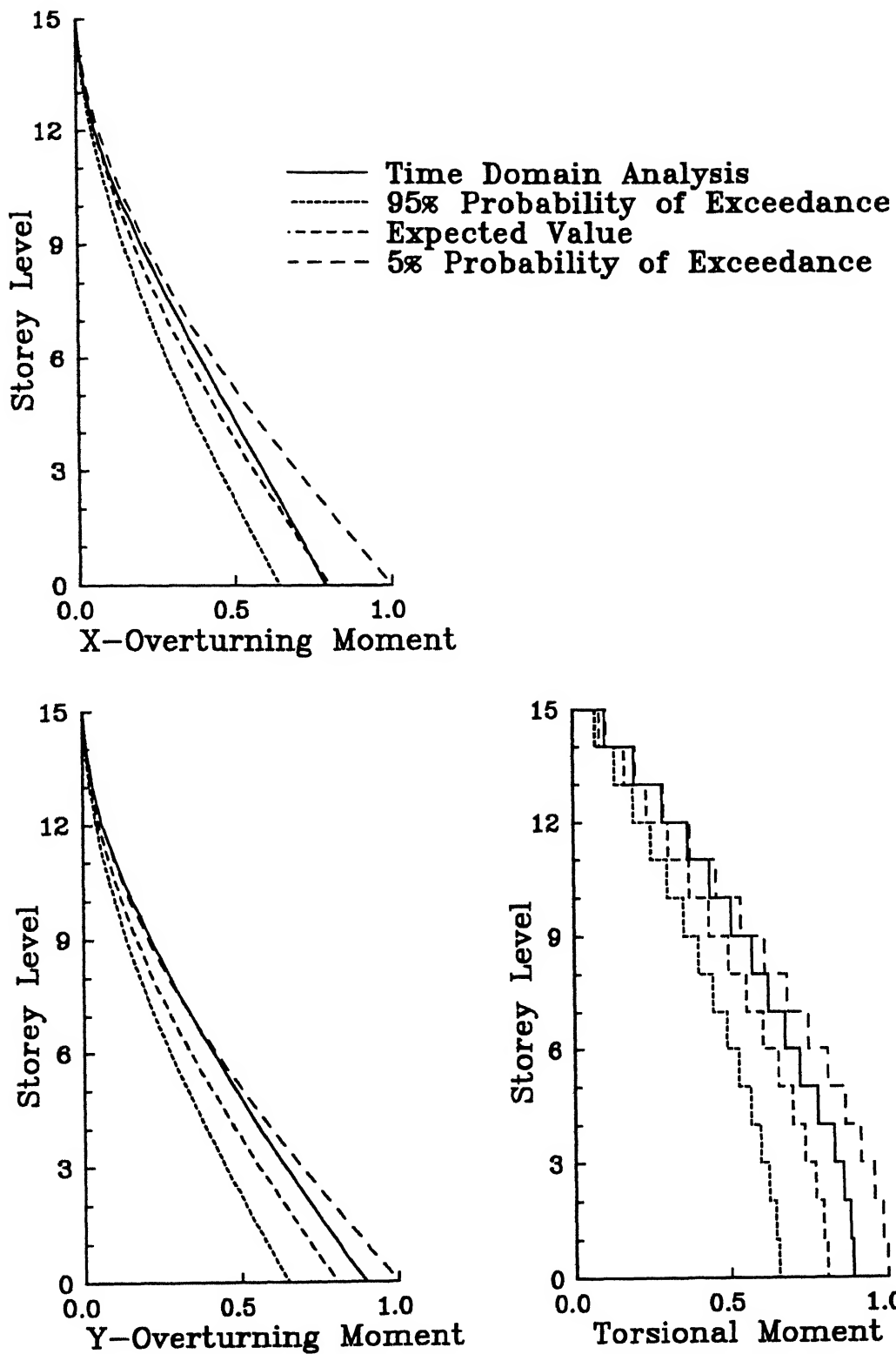


Figure 2.15 Normalized Moment Responses in Second Example Building for Imperial Valley Earthquake.

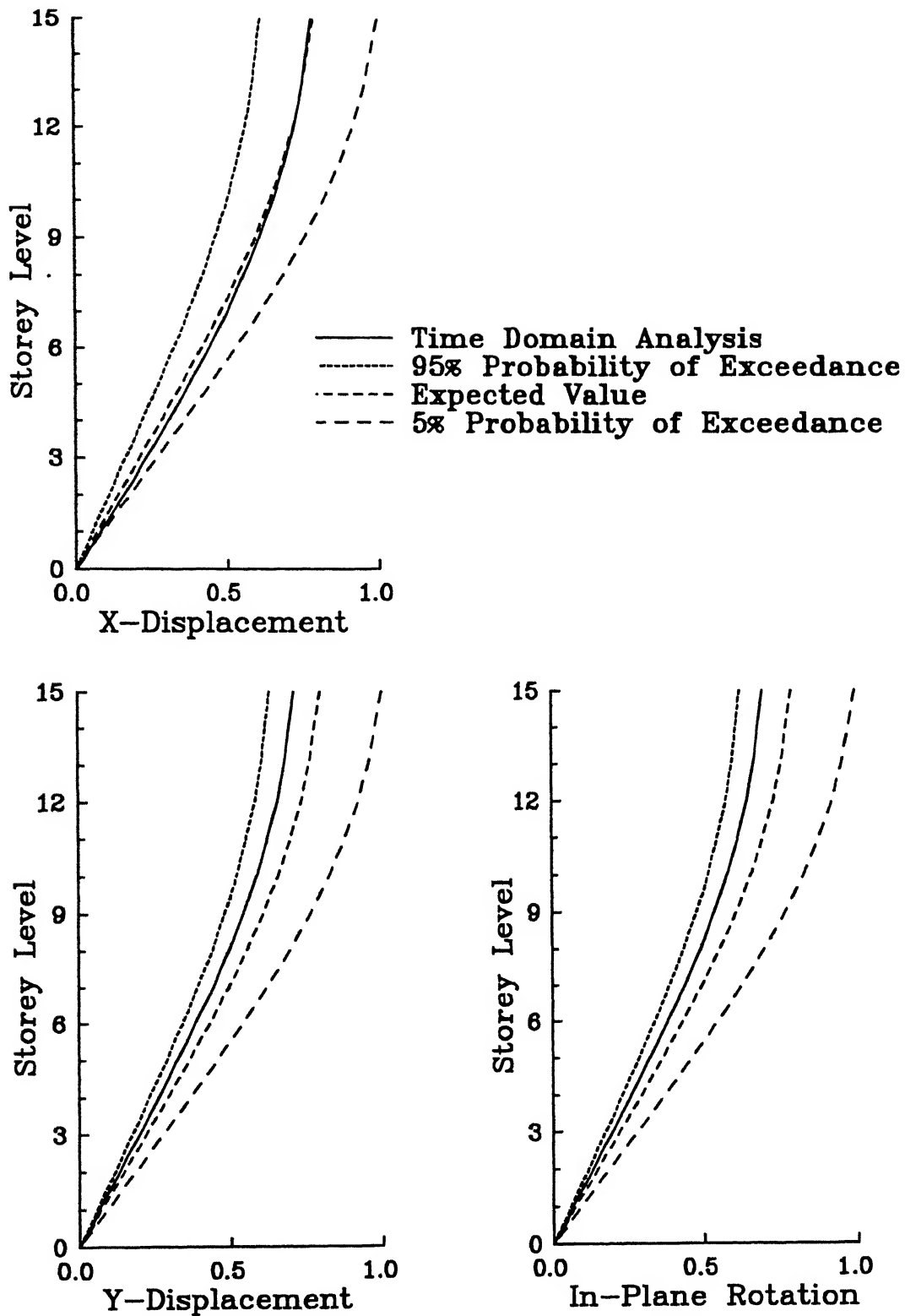


Figure 2.16 Normalized Displacement Responses in Second Example Building for Mexico Earthquake.

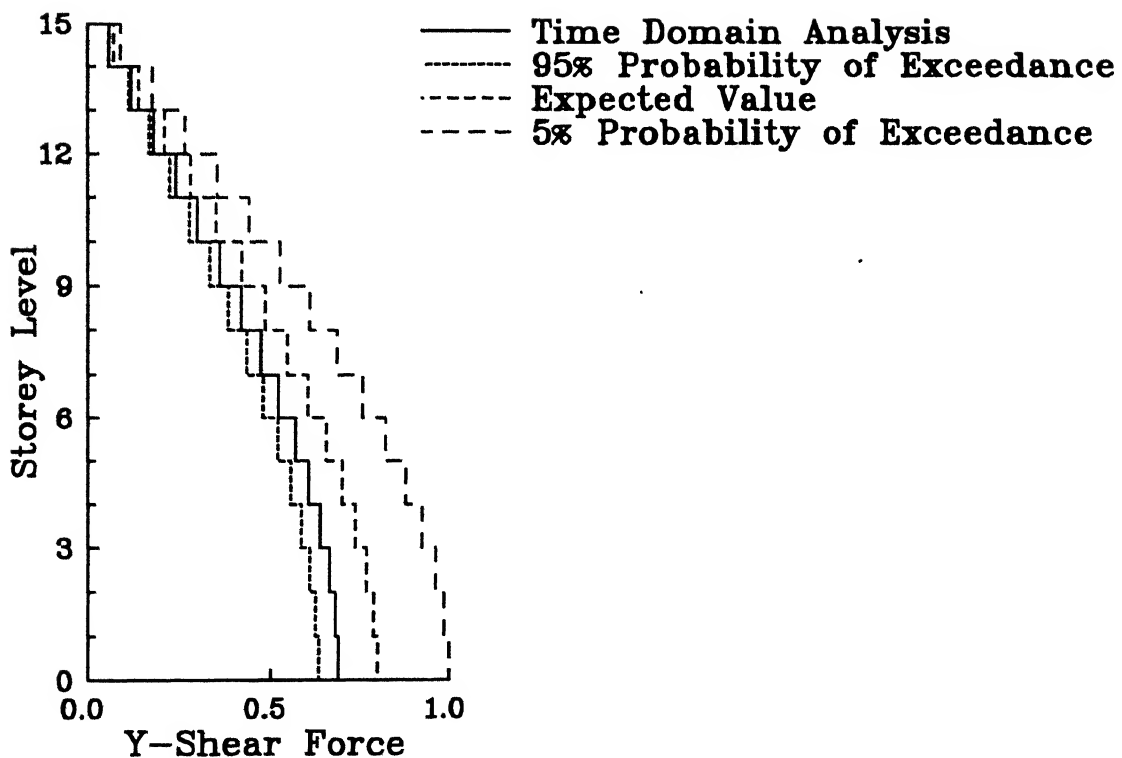
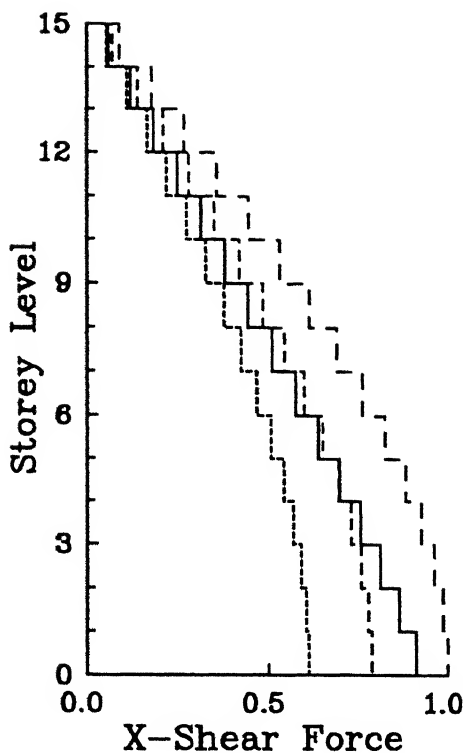


Figure 2.17 Normalized Shear Responses in Second Example Building for Mexico Earthquake.

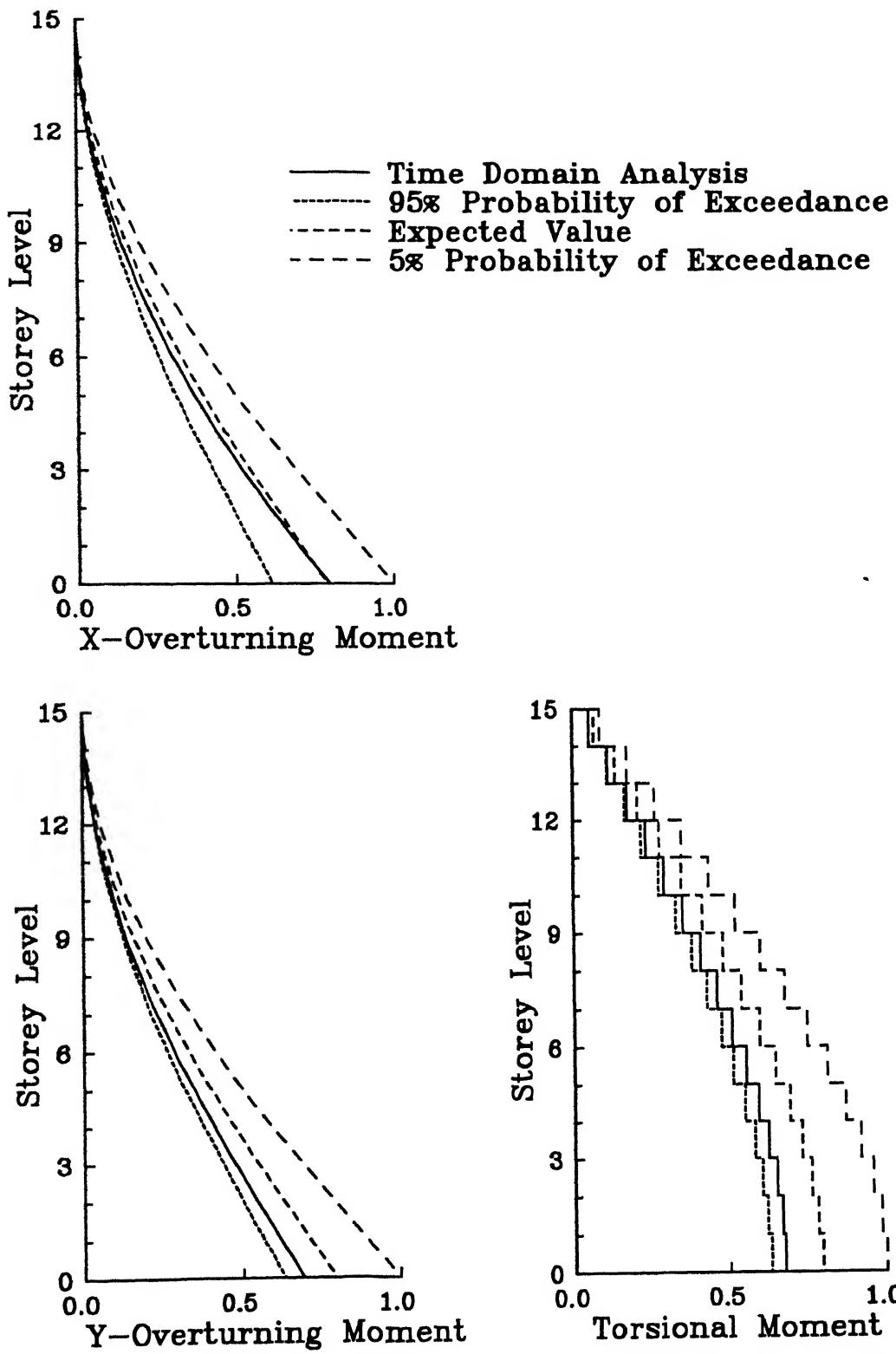


Figure 2.18 Normalized Moment Responses in Second Example Building for Mexico Earthquake.

CHAPTER III

DYNAMIC AMPLIFICATION OF ECCENTRICITY

USING STOCHASTIC APPROACH

3.1 Background

Due to the complexities and cost involved in analysing structures for the seismic loading, simplified approaches based on equivalent static load qualification have been adopted in design practices all over the world. The concept of dynamic eccentricity and associated dynamic amplification of static eccentricity forms a major component of various code provisions to account for the torsional effects in unsymmetric buildings. The stochastic approach presented in Chapter II can be conveniently employed to study the variation of dynamic amplification of eccentricity for various parameters, and thus to critically examine the conservatism involved in these code provisions.

3.2 Dynamic Amplification of Eccentricity

Various investigators have shown that the torsional coupling due to static eccentricity in an unsymmetrical building causes dynamic torque about the centre of resistance and reduces the storey shears. Modern building codes consider the design storey torque, T_d as

$$T_d = T_e + T_a \quad (3.2.1)$$

where, T_e is due to the static eccentricity and T_a is considered additionally to account for the effect of accidental eccentricity. Thus, even the symmetric buildings are designed for the application of lateral loads and torsional moments at

each storey. The design torque at each storey is obtained by multiplying the storey shear by a quantity termed as design eccentricity, e where

$$e = e_d + e_a \quad . \quad (3.2.2)$$

Here, the first part, e_d , is called dynamic eccentricity and it is a function of static eccentricity (the distance between centre of mass and centre of resistance). The dynamic eccentricity, e_d , is defined as the distance measured from the centre of rigidity at which static shear (obtained from the dynamic analysis while ignoring the rotational degree-of-freedom) should act in order to give rise to the same torque as that obtained by dynamic analysis for the torsionally coupled system. The second part, e_a , commonly referred to as accidental eccentricity, accounts for other factors such as torsional component of ground motion and the unforeseen differences between actual and computed static eccentricities. The accidental eccentricity is expressed as a function of the plan dimensions of the building. This has been ignored in the present investigation in order to emphasize the parametric variation of dynamic eccentricity alone.

The formulation presented in Chapter II for the seismic response of a torsionally coupled multistoreyed building will be used here to obtain the expected values of the largest torque response peaks at various floor levels. Let the torque amplitude, acting about the centre of resistance, at the i^{th} storey be denoted as T_{Ri} , $i = 1, 2 \dots n$. If V_{X0i} is the expected value of the largest storey shear at the i^{th} storey ignoring the torsional coupling (i.e. by taking $e_{X_i} = 0$, $e_{Y_i} = 0$, $i = 1, 2, \dots, n$), the dynamic eccentricity e_{di} at the i^{th} floor level becomes

$$e_{di} = \frac{T_{Ri}}{V_{X0i}} \quad . \quad (3.2.3)$$

The dynamic eccentricity is generally expressed as a dimensionless quantity, called as dynamic eccentricity ratio, e_{dri} , and is given by

$$e_{dri} = \frac{e_{di}}{r_i} \quad (3.2.4)$$

where, r_i is the radius of gyration of the i^{th} floor. The dynamic amplification of eccentricity, γ_i (henceforth to be called as amplification factor) will thus be given by

$$\gamma_i = \frac{e_{dri}}{e_{ri}} \quad , \quad (3.2.5)$$

where e_{ri} ($= e_i/r_i$) is the static eccentricity ratio. The eccentricity, e_i here is measured perpendicular to the direction of earthquake excitation.

3.3 Example Analysis

To study the variation of dynamic amplification of eccentricity in a multistoreyed building, a 8-storey fixed-base torsionally coupled multistorey building has been considered here. The building has a uniform floor dimension of 20 m x 25 m and a constant storey height of 3.75 m. The critical damping ratio has been assumed equal to 0.05 in all the modes. The natural frequencies of the corresponding torsionally uncoupled building are shown in Table 3.1. It may be observed from the table that the storey stiffnesses have been so adjusted that the uncoupled torsional and translational frequencies are same. To provide the base excitation to the building in X-direction, recorded ground motion of Imperial Valley Earthquake, May 18, 1940, at El Centro has been considered.

Table 3.1 - Natural Frequencies of Torsionally Uncoupled Building

Mode #	ω_X (rad/sec)	ω_Y (rad/sec)	ω_θ (rad/sec)
1	7.570	8.680	7.570
2	20.17	23.19	20.17
3	32.51	37.39	32.51
4	43.82	50.39	43.82
5	53.67	61.73	53.67
6	61.72	70.97	61.72
7	67.67	77.82	67.67
8	71.35	82.05	71.35

To investigate the effect of floor to floor variation of static eccentricity on the amplification factor, γ_i , five different cases have been considered:

Case I: Constant eccentricity ratio $e_{ri} = 0.1$ from top to bottom floor.

Case II: Step variation with $e_{ri} = 0.1$ for $i = 1, 2, 3, 4$ and $e_{ri} = 0.4$ for $i = 5, 6, 7, 8$.

Case III: Step variation with $e_{ri} = 0.1$ for $i = 1, 2, 3, 4$ and $e_{ri} = 0.025$ for $i = 5, 6, 7, 8$.

Case IV: Linear variation of e_{ri} from 0.1 at top to 0.025 at the bottom floor.

Case V: Linear variation of e_{ri} from 0.4 at bottom to 0.1 at the top floor.

It may be noted here that in all the above five cases, value of e_{ri} has been kept constant at 0.1 for $i = 1$. Further, the eccentricity in the direction of earthquake excitation is taken same as that in the perpendicular direction.

Fig. 3.1 shows the results of dynamic amplification of eccentricity for the above cases. It is observed that the dynamic amplification of eccentricity at the top storey is not significantly affected by the patterns of floor eccentricity variations in various example cases. Moreover, γ_i consistently decreases/increases with the increase/decrease in e_{ri} and remains constant in the case of same eccentricity ratio at different floors. This shows that the dynamic amplification of eccentricity at a given floor level is almost independent of the eccentricities at the other floors, and it is rather dependent on the static eccentricity at the same floor level. Further, the variation of dynamic eccentricity ratio is not linear in Cases IV and V, and therefore, γ_i does not seem to vary linearly with the variation in static eccentricity. This also suggests that it will be possible to estimate the dynamic eccentricity ratio at any floor of a multistoreyed building from the knowledge of its static eccentricity and that of the variation of dynamic eccentricity with the static eccentricity. In what follows, a single storey building model will be considered to investigate the possibility of estimating the relation between e_{dr} and e_r in case of a typical floor of a multistoreyed building by using the parallel results of a single storey model.

The relation between the dynamic eccentricity and the static eccentricity in case of a multistoreyed building is estimated here by considering the Case I above. In the corresponding torsionally uncoupled multistorey building, let ω_{X1} be the fundamental translational frequency of vibration in X-direction, ω_{Y1} be

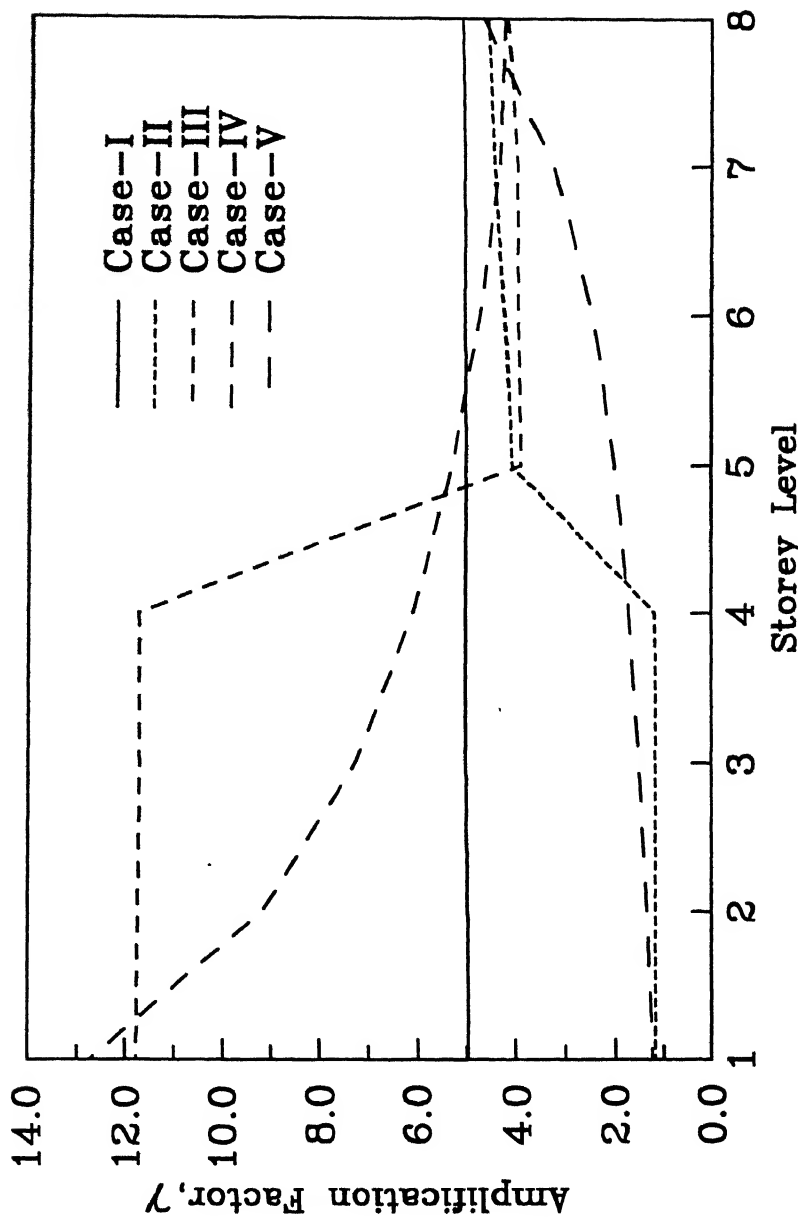


Figure 3.1 Effect of Floor Variation of Eccentricity on Amplification Factor.

the fundamental frequency in Y-direction, and $\omega_{\theta 1}$ be the fundamental frequency in torsional vibration. The single storey system is now considered to have the same natural translational and torsional frequencies i.e. ω_{X1} , ω_{Y1} and $\omega_{\theta 1}$. Thus, the single storey model has following properties:

- i) mass of the floor, $m = 73272 \text{ kg}$
- ii) translational stiffness in X-direction, $K_X = m \omega_{X1}^2 = 4.2 \times 10^6 \text{ N/m}$
- iii) translational stiffness in Y-direction, $K_Y = m \omega_{Y1}^2 = 5.52 \times 10^6 \text{ N/m}$
- iv) torsional stiffness about the centre of mass, $K_\theta = m \omega_{\theta 1}^2 r^2$
 $= 358.7 \times 10^6 \text{ Nm/rad.}$

Dynamic amplification of eccentricity in the above two models is obtained for the static eccentricity ratio varying from 0.05 to 0.4 as shown in Fig. 3.2. Results for the multistorey building model as presented in the figure have been obtained by averaging the dynamic amplification factors for different floor levels. It is seen that the two curves are in excellent agreement over the range of eccentricity ratio considered. This behaviour is also observed in a 13-storey building with same storey height, floor dimensions and damping ratios (see Fig. 3.3). This clearly shows that it suffices to analyze a single storey building and to obtain the curve as in Fig. 3.2 to estimate the storey torque at any floor of a torsionally coupled multistoreyed building. It is also seen from Fig. 3.2 that the dynamic eccentricity ratio decreases nonlinearly with the increase in the static eccentricity ratio. This is in conformity with the observations from Fig. 3.1 and with the findings of earlier research work e.g. Tso and Dempsey (1980), Tsienias and Hutchinson (1981) and Chandler and Hutchinson (1988).

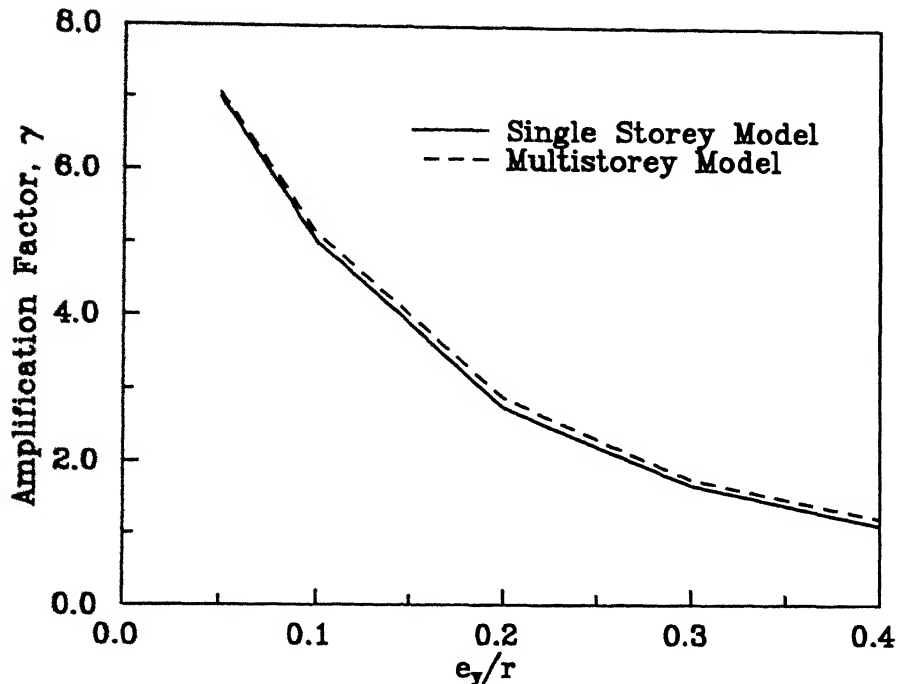


Figure 3.2 Comparison of Amplification Factor in 1 and 8-Storey Buildings.

REF ID: A115712
Doc. No. A115712

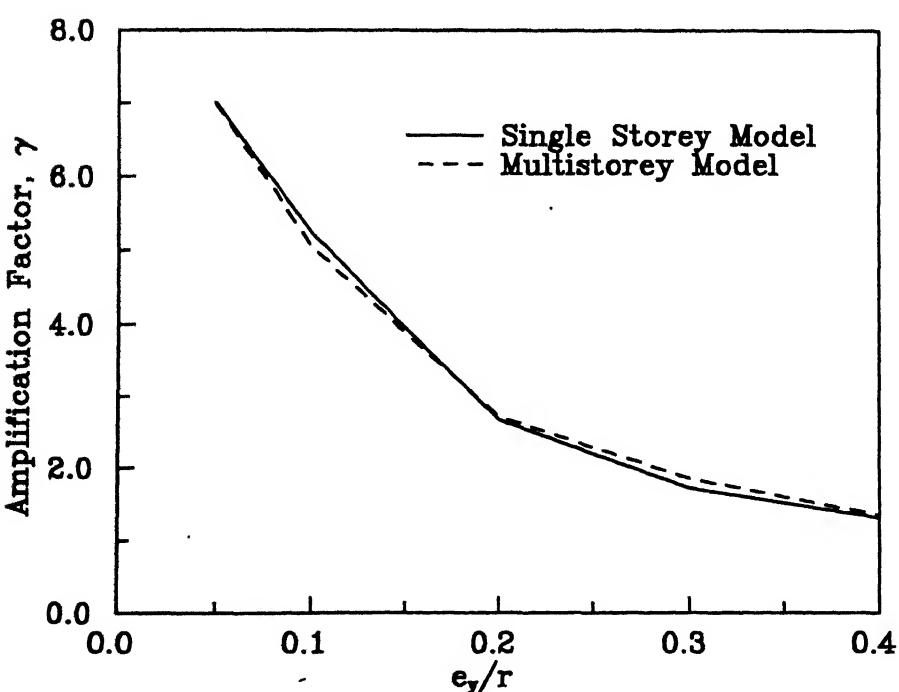


Figure 3.3 Comparison of Amplification Factor in 1 and 13-Storey Buildings.

3.4 Parametric Dependence of Amplification Factor

In what follows, single storey models will be considered to study the dependence of dynamic amplification of eccentricity i.e. γ on i) earthquake excitation, ii) uncoupled frequency ratio, ω_θ/ω_X , and on iii) eccentricity in X-direction. For the reasons discussed above, the results and inferences obtained in the parametric study will also be applicable to the multistoreyed buildings.

i) Effect of Earthquake Excitation

The variation of γ for the same example single storey model as considered above is shown in Fig. 3.4 for the three base excitations; a) S00E Component of Imperial Valley Earthquake, May 18, 1940, at El Centro; b) N85E Component of California Earthquake, June 27, 1966, at Parkfield; c) Mexico Earthquake, 1985, synthetically generated for Mexico City Site (see Gupta and Trifunac (1990c)). It is seen from the figure that the characteristics of the input excitation, have negligible effect on the dependence of γ on static eccentricity.

ii) Effect of Uncoupled Frequency Ratio

The dependence of amplification factor, γ variation with static eccentricity ratio on ω_θ/ω_X is shown in Fig. 3.5 by considering the example single storey building with $\omega_\theta/\omega_X = 0.7, 0.9, 1.0, 1.1, 1.3$. It is seen in the figure that, for moderate and large static eccentricity ratios, the amplification factor, γ tends asymptotically to a constant value for all the values of ω_θ/ω_X considered. Also, at small eccentricities, the amplification factor becomes maximum for the case of torsional frequency being nearly equal to the translational frequency. These

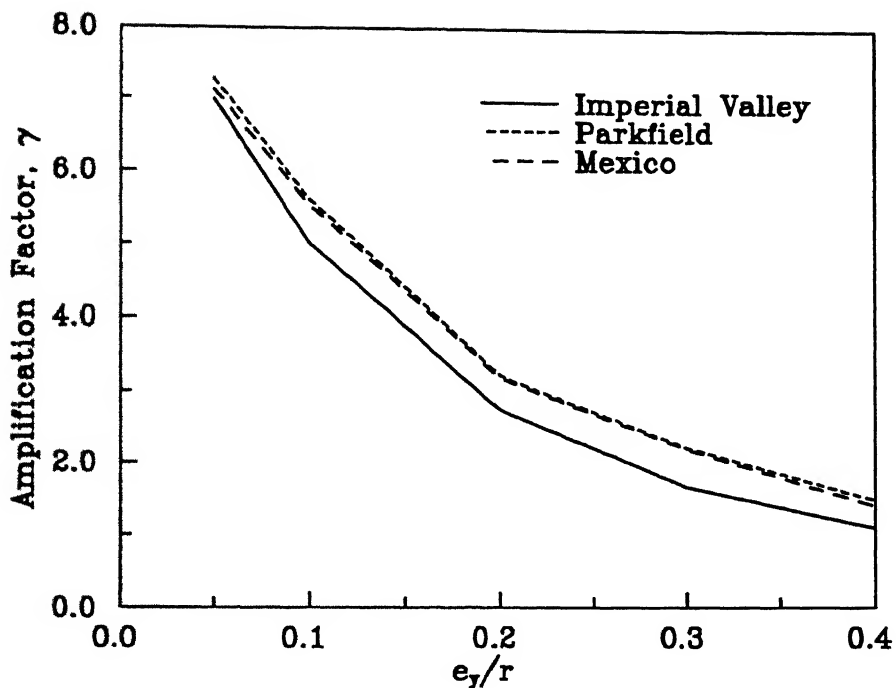


Figure 3.4 Effect of Different Earthquake Excitations on Amplification Factor.

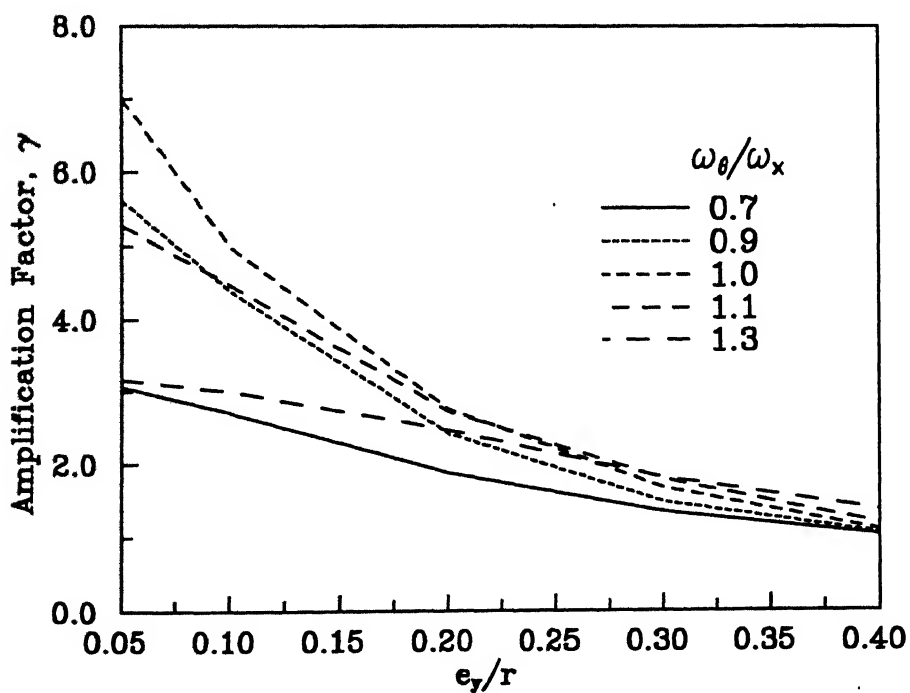


Figure 3.5 Variation of Amplification Factor with e_y/r for Different ω_θ/ω_x Values.

results are in agreement with those by Tsienias and Hutchinson (1981), Kung and Pecknold (1984), Chandler and Hutchinson (1986) and Rady and Hutchinson (1988). To see this behaviour more clearly, the above results have also been obtained as shown in Fig. 3.6. It can be seen that the curves for small eccentricity ratios i.e. $e/r = 0.05$ and 0.1 have distinct peaks in the vicinity of $\omega_\theta/\omega_X = 1.0$, and for moderate and large eccentricities, there is little effect of the uncoupled frequency ratio. Moreover, for all the eccentricity ratios, the effect of torsional to translational frequency ratio on γ becomes negligible as these frequency grow apart. Then it may be possible to approximate γ by constant values which are functions of e/r only.

iii) Effect of Eccentricity Ratio in X-direction

The effect of eccentricity ratio, e_{Xr} , in the direction of base excitation, has been shown in Fig. 3.7 by considering the example single storey building and by plotting the curves for the eccentricity ratio $e_{Yr} = 0.05, 0.1, 0.2$ and 0.4 . Each curve shows the variation of dynamic amplification of eccentricity with the eccentricity ratio e_{Xr} as a fraction of e_{Yr} . It appears that the amplification factor γ varies little with the eccentricity in the direction of excitation and that it becomes maximum in the case of zero value of e_{Xr} . Thus it may be justified to estimate the critical values of dynamic eccentricity by ignoring the static eccentricity in the direction of excitation.

3.5 Comparison with Indian Standard Code Provisions

As shown above, it is obvious that the amplification factor is maximum

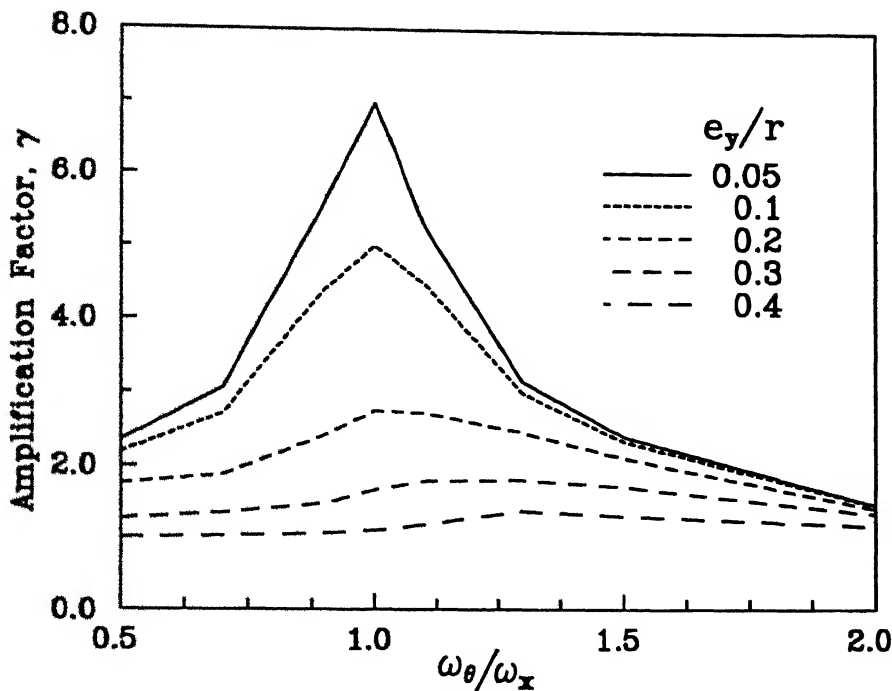


Figure 3.6 Variation of Amplification Factor with ω_θ/ω_x for Different e_y/r Values.

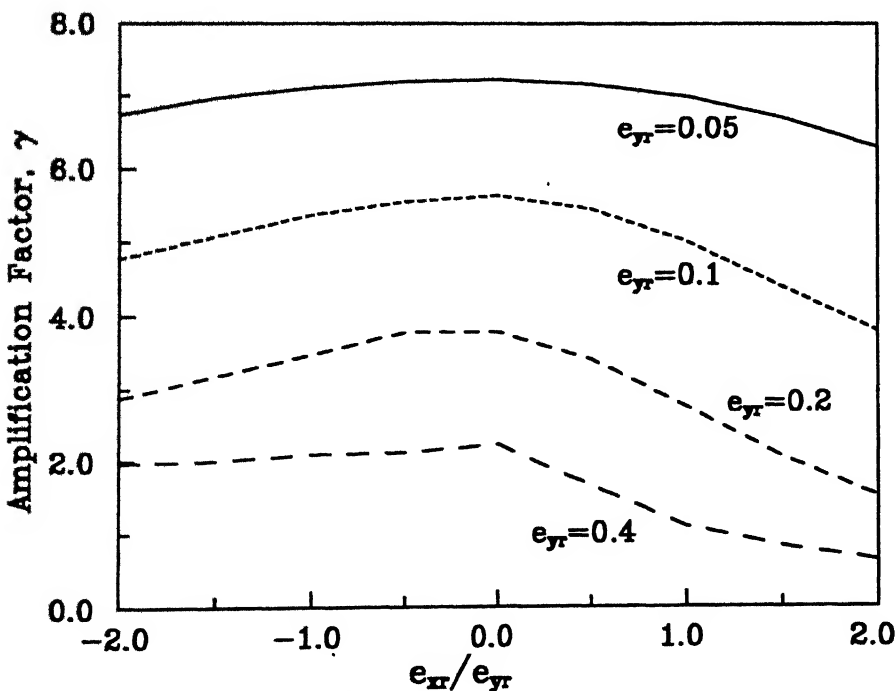


Figure 3.7 Effect of e_{xx} on Amplification Factor for Different e_{yr} Values.

when the static eccentricity occurs only in the perpendicular direction of excitation and its component in the orthogonal direction is zero. To critically examine the seismic code provisions, therefore, the example single storey model has been considered with eccentricity only in the perpendicular direction of excitation, and its results on the dynamic eccentricity have been compared with those recommended by the code (IS: 1893-1984) as shown in Fig. 3.8. The code recommends the dynamic eccentricity as $1.5e$, where e is the computed static eccentricity. The figure clearly indicates that for all the values of ω_θ/ω_X considered in the range of 0.7-1.3, the code severely underestimates the dynamic amplification of eccentricity for small values of eccentricities. However, for large values, codal provisions are slightly on the unsafe side. It is also clear that the code does not account for the significant effects of ω_θ/ω_X . In case of torsional coupling in a building, if the torsional frequencies are very close to the translational frequencies and also if the static eccentricities are very small, the actual dynamic eccentricities may be as much as five times that recommended by the code. To appreciate this point more clearly, the variation of amplification factor with e/r , has been shown in Fig. 3.9 for 1st, 4th, 7th, 10th and 15th orders of peak in case of the example single storey model (with $\omega_\theta/\omega_X = 1$). It is seen that for the small to moderate eccentricities, even the 15th order peak of dynamic eccentricity ratio is larger than the values recommended by the code. Thus, there appears to be a very high demand of ductility for the building designed as per the code. In other words, the torsionally coupled building with the usually provided levels of ductility are unsafe against the actual storey torques in critical cases when they are designed as per IS: 1893-1984.

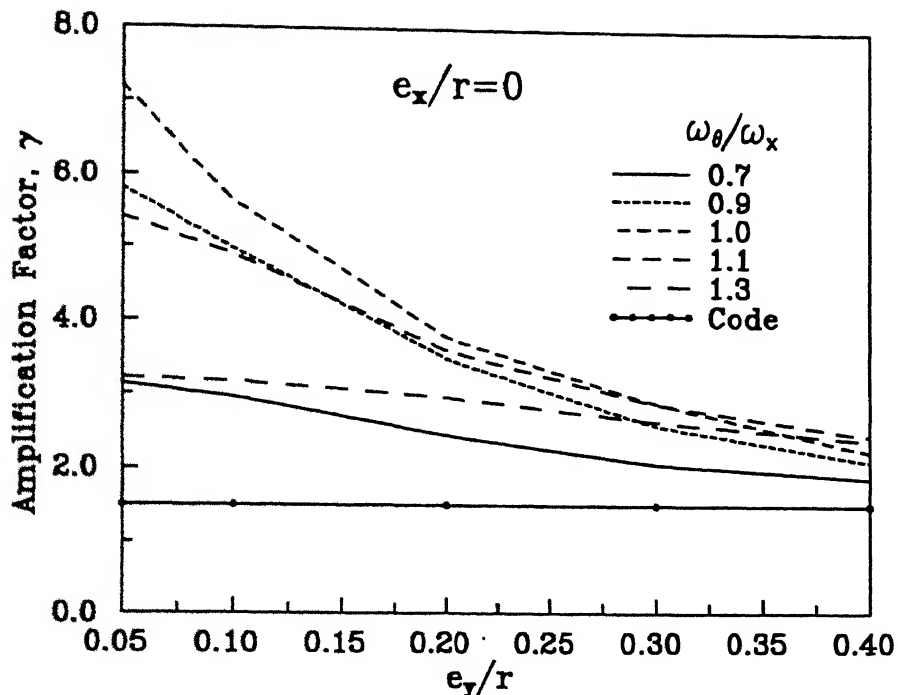


Figure 3.8 Comparison of Amplification Factor with the Code Values.

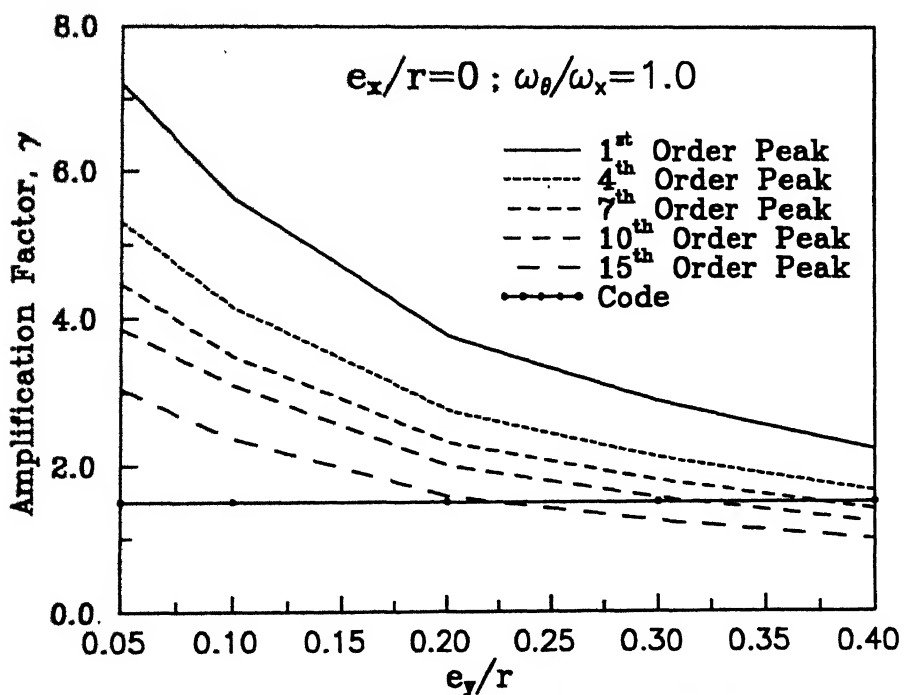


Figure 3.9 Comparison of Amplification Factor for Higher Orders of Peak with the Code Values.

CHAPTER IV

CONCLUSIONS

A response spectrum based stochastic approach has been formulated for the seismic response of fixed-base torsionally coupled multistoreyed buildings. This approach uses the information available from the Fourier synthesis of the ground motion, and from this, the estimates of response peaks for all orders can be obtained with the desired level of confidence. Thus, it is possible to obtain the expected peak values of any response function, and thus to get an idea about the 'average' values which the response function may assume during the life time of the building. Further, depending on the importance of the structure and its intended life, suitable design values can be obtained by choosing an appropriate probability of exceedance. The presented formulation is quite general as it accounts for the cross-correlation between various modes of vibration. This includes the cases of closely spaced modes and those cases in which the structure is too stiff with respect to the ground motion. It has been seen that this approach gives reasonably good estimates in case of the considered example buildings and excitations.

The proposed approach has been used to study the dynamic amplification of eccentricity due to torsional coupling by determining the dynamic eccentricities based on the expected first order peak amplitudes of storey torques and shears. On the basis of this, a simple and generalized procedure has been illustrated to estimate the dynamic amplification values of eccentricity at different floor levels of a torsionally coupled multistoreyed building. In this procedure, one

needs to analyze an 'equivalent' single storey model only. It has been found that these amplification factors are not much affected by the excitation characteristics and are strongly dependent on the ratio of uncoupled torsional frequency to the uncoupled translational frequency.

A comparison of the single storey results with the seismic code provisions has shown that the code severely underestimates the torsional moments, particularly when the eccentricities of the building are small and when the uncoupled frequency ratio of the building is close to unity. Even in this case when the eccentricity is moderate, say 0.2, the code estimates are as low as the 15th order peak of the torsional response. This means that in such a case, the torsional response is likely to exceed the value prescribed by the code about 15 times during the earthquake excitation. Since the code provisions are designed to provide simple but conservative estimates of the torsional moments in asymmetrical structures, a more comprehensive study of the dynamic eccentricity is needed to be carried out for the desired revisions in the codal provisions. It will also be desirable to work, in these revisions, towards the simplified formulae for dynamic eccentricity which will allow the dependence of dynamic eccentricity on the static eccentricity and on the ratio of torsional to translational frequency.

REFERENCES

Amini, A. and M.D. Trifunac (1981). Distribution of peaks in linear earthquake response, *J. Eng. Mech. Div., Proc. ASCE* 107(EM1), 207-227.

Amini, A. and M.D. Trifunac (1985). Statistical extension of response spectrum superposition, *Soil Dyn. Earthq. Eng.* 4(2), 54-63.

Bustamante, J.I. and E. Rosenblueth (1960). Building code provisions on torsional oscillations, *Proc. Second Wld Conf. Earthq. Eng., Japan*, 2, 879-894.

Cartwright, D.E. and M.S. Longuet-Higgins (1956). The statistical distribution of maxima of a random function, *Proc. Roy. Soc. London A* 237, 212-232.

Caughey, T.K. and A.H. Gray (1963). Discussion: distribution of structural response to earthquakes, *J. Eng. Mech. Div., Proc. ASCE* 89(EM2), 159-168.

Chandler, A.M. (1986). Building damage in Mexico City earthquake, *Nature* 320(6062), 497-501.

Chandler, A.M. and G.L. Hutchinson (1986). Seismic design eccentricity for torsionally coupled building, *Proc. Eighth Eur. Conf. Earthq. Eng., Lisbon*, 6(7), 33-40.

Chandler, A.M. and G.L. Hutchinson (1987). Evaluation of code torsional provisions by a time history approach, *Earthq. Eng. Struct. Dyn.* 15, 491-516.

Chandler, A.M. and G.L. Hutchinson (1988). Evaluation of the secondary torsional design provisions of earthquake building codes, *Proc. Instn. Civ. Engrs., London, Part 2(85)*, 587-607.

David, F.N. and N.L. Johnson (1954). Statistical treatment of censored data, Part I: Fundamental formulae, *Biometrika* 41, 228-240.

Dempsey, K.M. and H.M. Irvine (1979). Envelopes of maximum seismic response for a partially symmetric single-storey building model, *Earthq. Eng. Struct. Dyn.* 7, 161-180.

Dempsey, K.M. and W.K. Tso (1982). An alternative path to seismic torsional provisions, *Soil Dyn. Earthq. Eng.* 1(1), 3-10.

Douglas, B.M. and T.E. Trabert (1973). Coupled torsional dynamic analysis of a multistory building, *Bull. Seism. Soc. Amer.* 63(3), 1025-1039.

Esteva, L., O.A. Rascon and A. Gutierrez (1969). Lessons from some recent earthquakes in Latin America, *Proc. Fourth Wld Conf. Earthq. Eng., Santiago, Chile*, 3(J-2), 58-73.

Gasparini, D.A. (1979). Response of MDOF systems to nonstationary random excitation, *J. Eng. Mech. Div., Proc. ASCE* 105(EM1), 13-27.

Gibson, R.E., M.L. Moody and R.S. Ayre (1972). Response spectrum solution for earthquake analysis of unsymmetrical multistoried building, *Bull. Seism. Soc. Amer.* 62, 215-229.

Gluck, J., A. Reinhorn and A. Rutenberg (1979). Dynamic torsional coupling in tall building structures, *Proc. Instn. Civil Engrs. Part 2(67)*, 411-425.

Gupta, I.D. and M.D. Trifunac (1987a). A note on contribution of torsional excitation to earthquake response of simple symmetric buildings, *Earthq. Eng. Vib.* 7(3), 27-46.

Gupta, I.D. and M.D. Trifunac (1987b). Order statistics of peaks in earthquake response of multi-degree-of-freedom systems, *Earthq. Eng. Eng. Vib.* 7(4), 15-50.

Gupta, I.D. and M.D. Trifunac (1988). Order statistics of peaks in earthquake response, *J. Eng. Mech.* 114(10), 1605-1627.

Gupta, V.K. and M.D. Trifunac (1990a). Response of multistoried buildings to ground translation and torsion during earthquakes, *European Earthq. Eng.* IV(1), 34-42.

Gupta, V.K. and M.D. Trifunac (1990b). A note on contribution of ground torsion to seismic response of symmetric multistoried buildings, *Earthq. Eng. Eng. Vib.* 10(3), 27-40.

Gupta, V.K. and M.D. Trifunac (1990c). Response of multistoried buildings to ground translation and rocking during earthquakes, *J. Prob. Eng. Mech.* 5(3), 138-145.

Gupta, V.K. and M.D. Trifunac (1992). Higher order peaks in response of multistoried buildings, *Proc. Tenth Wld Conf. Earthq. Eng., Madrid, Spain*, 3819-3824.

Hadjian, A.H. (1981). Seismic response of structures by the response spectrum methods, *Nucl. Eng. Design* 66, 179-201.

Hammond, J.K. (1968). On the response of single and multidegree of freedom systems to non-stationary random excitations, *J. Sound Vib.* 7(3), 393-416.

Hart, G.C., R.M. DiJulio, Jr. and M. Lew (1975). Torsional response of high-rise buildings, *J. Struct. Div., Proc. ASCE* 101(ST2), 397-416.

Hejal, R. and A.K. Chopra (1989a). Earthquake analysis of a class of torsionally-coupled buildings, *Earthq. Eng. Struct. Dyn.* 18, 305-323.

Hejal, R. and A.K. Chopra (1989b). Earthquake response of torsionally coupled, frame buildings, *J. Struct. Eng.* 115(4), 834-851.

Housner, G.W. and H. Outinen (1958). The effects of torsional oscillations on earthquake stresses, *Bull. Seism. Soc. Amer.* 48(2), 221-229.

Huckelbridge, A.A. and E.Y.H. Lei (1986). Torsional seismic load effects in nearly symmetric structures, *Proc. Eighth Eur. Conf. Earthq. Eng., Lisbon*, 6(7), 41-48.

Hutchinson, G.L. and A.M. Chandler (1986). Parametric earthquake response of torsionally coupled buildings and comparison with building codes, *Proc. Eighth Eur. Conf. Earthq. Eng., Lisbon*, 6(7), 25-32.

Hutchinson, G.L., A.M. Chandler and M.A. Rady (1991). Effect of vertical distributions of mass and translational stiffness on dynamic eccentricities for a special class of multi-storey buildings, *Pacific Conf. Earthq. Eng., New Zealand*, f 1, 61-69.

IS: 1893-1984. Criteria for earthquake resistant design of structures, *Bureau of Indian Standards, New Delhi*.

Kan, C.L. and A.K. Chopra (1977a). Effects of torsional coupling on earthquake forces in buildings, *J. Struct. Div., Proc. ASCE* 103(ST4), 805-819.

Kan, C.L. and A.K. Chopra (1977b). Elastic earthquake analysis of a class of torsionally coupled buildings, *J. Struct. Div., Proc. ASCE* 103(ST4), 821-838.

Kan, C.L. and A.K. Chopra (1977c). Elastic earthquake analysis of torsionally coupled multistorey buildings, *Earthq. Eng. Struct. Dyn.* 5, 395-412.

Kan, C.L. and A.K. Chopra (1981a). Simple model for earthquake response studies of torsionally coupled buildings, *J. Eng. Mech. Div., Proc. ASCE* 107(EM5), 935-951.

Kan, C.L. and A.K. Chopra (1981b). Torsional coupling and earthquake response of simple elastic and inelastic systems, *J. Struct. Div., Proc. ASCE* 107(ST8), 1569-1588.

Kaul, M.K. (1978). Stochastic characterization of earthquakes through their response spectrum, *Earthq. Eng. Struct. Dyn.* 6, 497-509.

Keintzel, E. (1973). On the seismic analysis of unsymmetrical storied buildings, *Proc. Fifth. Wld Conf. Earthq. Eng., Rome* Paper 10, 110-113.

Kiureghian, A.D. (1980). Structural response to stationary excitation, *J. Eng. Mech. Div., Proc. ASCE* 106(EM6), 1195-1213.

Kiureghian, A.D. (1981). A response spectrum method for random vibration analysis of MDF systems, *Earthq. Eng. Struct. Dyn.* 9, 419-435.

Kung, S.Y. and D.A. Pecknold (1984). Seismic response of torsionally coupled single-storey structures, *Proc. Eighth Wld Conf. Earthq. Eng., San Francisco, California*, 235-242.

Lam, P.C. and R.J. Scavuzzo (1981). Lateral-torsional structural response from free-field ground motion, *Nucl. Eng. Design* 65, 269-281.

Lin, A.N. (1989). Torsional response of symmetric structures, *J. Eng. Mech.* 115(2), 231-246.

Luco, J.E. (1976). Torsional response of structures to obliquely incident seismic SH waves, *Earthq. Eng. Struct. Dyn.* 4, 207-219.

Maheri, M.R., A.M. Chandler and R.H. Bassett (1991). Coupled lateral-torsional behaviour of frame structures under earthquake loading, *Earthq. Eng. Struct. Dyn.* 20, 61-85.

Medearis, K. (1966). Coupled bending and torsional oscillations of a modern skyscraper, *Bull. Seism. Soc. Amer.* 56(4), 937-946.

Mohraz, B. and F.E. Elghadamsi (1989). Earthquake ground motion and response spectra, *Seismic Design Handbook*, Van Nostrand Reinhold, New York, 32-80.

Newmark, N.M. (1969). Torsion in symmetrical buildings, *Proc. Fourth Wld Conf. Earthq. Eng., Santiago, Chile*, II(A-3), 19-32.

Penzien, J. (1969). Earthquake response of irregularly shaped buildings, *Proc. Fourth Wld Conf. Earthq. Eng., Santiago, Chile*, II(A-3), 75-89.

Rady, M.A. and G.L. Hutchinson (1988). Evaluation of dynamic eccentricities obtained using a probabilistic approach, response spectrum methods and modern building codes, *Earthq. Eng. Struct. Dyn.* 16, 275-291.

Rice, S.O. (1944). Mathematical analysis of random noise, *Bell Syst. Tech. J.* 23, 282-332.

Rice, S.O. (1945). Mathematical analysis of random noise, *Bell Syst. Tech. J.* **24**, 46-156.

Rosenblueth, E. and J. Elorduy (1969). Response of linear systems to certain transient disturbance, *Proc. Fourth Wld Conf. Earthq. Eng., Santiago, Chile*, **1(A-1)**, 185-196.

Rosenblueth, E. (1979). Seismic design requirements in the Mexican 1976 Code, *Earthq. Eng. Struct. Dyn.* **7**, 49-61.

Ruiz, P. and J. Penzien (1971). Stochastic seismic response of structures, *J. Struct. Div., Proc. ASCE* **97(ST4)**, 441-456.

Rutenberg, A., T.-I. Hsu and W.K. Tso (1978). Response spectrum techniques for asymmetric buildings, *Earthq. Eng. Struct. Dyn.* **6**, 427-435.

Shibata, A., J. Onose and T. Shiga (1969). Torsional response of buildings to strong earthquake motions, *Proc. Fourth Wld Conf. Earthq. Eng., Santiago, Chile*, **II(A-4)**, 123-138.

Shiga, T. (1965). Torsional vibrations of multistoried buildings, *Proc. Third Wld Conf. Earthq. Eng., New Zealand* **2**, 569-584.

Singh, M.P. and S.L. Chu (1976). Stochastic considerations in seismic analysis of structures, *Earthq. Eng. Struct. Dyn.* **4**, 295-307.

Tajimi, H. (1960). A statistical method of determining the maximum response of a building structure during an earthquake, *Proc. Second Wld Conf. Earthq. Eng., Tokyo, Japan*, **2**, 781-797.

Trifunac, M.D. and A.G. Brady (1975). A study on the duration of strong earthquake ground motion, *Bull. Seism. Soc. Amer.* **65(3)**, 581-626.

Tsienias, T.G. and G.L. Hutchinson (1981). Evaluation of code requirements for the earthquake resistant design of torsionally coupled buildings, *Proc. Instrn. Civ. Engrs. Part 2(71)*, 821-843.

Tsienias, T.G. and G.L. Hutchinson (1982a). Evaluation of code torsional provisions for earthquake resistant design of single storey buildings with two eccentricity components, *Proc. Instrn. Civ. Engrs. Part 2(73)*, 455-464.

Tsienias, T.G. and G.L. Hutchinson (1982b). A note on the perturbation analysis of the mode shapes of torsionally coupled buildings, *Earthq. Eng. Struct. Dyn.* **10**, 171-174.

Tso, W.K. (1975). Induced torsional oscillations in symmetrical structures, *Earthq. Eng. Struct. Dyn.* **3**, 337-346.

Tso, W.K. and T.-I Hsu (1978). Torsional spectrum for earthquake motions, *Earthq. Eng. Struct. Dyn.* **6**, 375-382.

Tso, W.K. and K.M. Dempsy (1980). Seismic torsional provisions for dynamic eccentricity, *Earthq. Eng. Struct. Dyn.* **8**, 275-289.

Tso, W.K. (1982). A proposal to improve the static torsional provisions for the National Building Code of Canada, *Can. J. Civ. Eng.* **10**(4), 561-565.

Tso, W.K. and V. Meng (1982). Torsional provisions in building codes, *Can. J. Civ. Eng.* **9**, 38-46.

Udwadia, F.E. and M.D. Trifunac (1973). Fourier transforms, response spectra and their relationship through the statistics of oscillator response, *Report EERL 73-01, California Institute of Technology, Pasadena, California*.

Udwadia, F.E. and M.D. Trifunac (1974). Characterization of response spectra through the statistics of oscillator response, *Bull. Seism. Soc. Amer.* **64**, 205-219.

Wittrick, W.H. and R.W. Horsington (1979). On the coupled torsional and sway vibrations of a class of shear buildings, *Earthq. Eng. Struct. Dyn.* **7**, 477-490.

Wu, S.T. and E.U. Leyendecker (1984). Dynamic eccentricity of structures subjected to SH-waves. *Earthq. Eng. Struct. Dyn.* **12**, 619-628.